UNIVERSITAT POLITÈCNICA DE VALÈNCIA

UNIVERSITAT POLITÈCNICA DE VALÈNCIA

Escuela Técnica Superior de Ingeniería Industrial

Electrification of high temperature heating demand: A techno-economic perspective on decarbonized steel making

Trabajo Fin de Master –Treball Final de Màster

Master Universitario en Ingeniería Industrial--Màster Universitari en Enginyeria Industrial

AUTOR: Oncina Micó, Ana

Tutores: Sarabia Escrivá; Emilio José; Laumert, Björn; Trevisan, Silvia; Rahman, Moksadur

CURSO ACADÉMICO: 2023/2024

KTH ROYAL INSTITUTE
OF TECHNOLOGY

30 credits

Electrification of High Temperature Heating Demand: A Techno-Economic Perspective on Decarbonized Steel Making

Ana Oncina Mico

Stockholm Sweden 2024

Abstract

Given the steel industry's status as the most carbon-intensive sector, significant efforts have been directed towards its decarbonization, primarily focusing on reducing emissions during the ironmaking phase, which accounts for 70% of the industry's total emissions. In contrast, this study addresses the decarbonization of the steelmaking and post-processing phases, which account for 30% of the industry's emissions and have been largely neglected until now.

This research presents a comprehensive review of existing literature on the decarbonization of the steel industry, followed by a comparative analysis of various electrification technologies and conventional methods, specifically targeting mini-mills. The study evaluates the energy intensity and emissions reduction potential of these electrification technologies. It examines the efficacy of preheating technologies for scrap entering the Electric Arc Furnace (EAF) and assesses the impact of different metal inputs on the EAF's energy balance. Additionally, the study investigates the potential of electrification technologies for the reheating furnace and conducts an economic analysis considering future trends such as carbon pricing and energy costs.

The findings indicate that electrification technologies offer a viable strategy for decarbonizing the steel industry. However, their effectiveness highly depends on the emissions profile of the electricity used to power the steel plants. Moreover, the economic viability of these technologies remains a significant challenge in the current context, underscoring the need for policy measures to facilitate the transition towards a sustainable steel industry.

Keywords

Steel, Mini-mill, Decarbonization, Electrification of heat, Energy modeling

Abstract

Som följd av stålindustrins status som den mest koldioxidintensiva sektorn har betydande ansträngningar gjorts för att minska utsläppen, främst genom förbättringar under järnframställningsfasen, som står för 70% av industrins totala utsläpp. I denna studie behandlas istället utfasningen av fossila bränslen i ståltillverknings- och efterbearbetningsfaserna, som står för 30% av industrins utsläpp och som hittills i stor utsträckning har försummats.

Arbetet presenterar en omfattande genomgång av befintlig litteratur om utfasning av fossila bränslen i stålindustrin, följt av en jämförande analys av olika elektrifieringstekniker och konventionella metoder, med särskild inriktning på minikvarnar. Studien utvärderar både energinivåer och potentialen för utsläppsminskning med dessa elektrifieringstekniker. Den undersöker också effektiviteten hos tekniker för förvärmning av det skrot som går in i ljusbågsugnen (EAF) och bedömer effekten av olika metallinmatningar på ljusbågsugnens energibalans. Dessutom undersöker studien potentialen för elektrifieringstekniker för återuppvärmningsugnen och genomför en ekonomisk analys med hänsyn till framtida trender som koldioxidprissättning och energikostnader.

Resultaten visar att elektrifiering är en genomförbar strategi för att minska koldioxidutsläppen inom stålindustrin. Hur effektiva dessa åtgärder är beror dock i hög grad på utsläppsprofilen för den el som används för att driva stålverken. Dessutom är den ekonomiska lönsamheten för dessa tekniker fortfarande en stor utmaning i dagsläget, vilket understryker behovet av politiska åtgärder för att underlätta övergången till en hållbar stålindustri.

Nyckelord

Stål, Miniverk, Utfasning av fossila bränslen, Elektrifiering av värme, Energimodellering

Acknowledgements

I would like to extend my heartfelt gratitude to my family for their unwavering support throughout college. Their encouragement has been greatly appreciated.

I am thankful to my supervisor, Moksadur Rahman, at ABB Corporate Research Center, for his guidance and support over these months. I also wish to express my sincere appreciation to my master thesis colleagues at ABB and the wonderful people I have met during my time at KTH. This journey has been a fantastic experience, and I am thankful for the opportunity to work with such talented individuals.

A special thank you to Silvia Trevissan, my supervisor at KTH, for her support during this time. I would also like to extend my appreciation to my examiner, Björn Laumert.

Authors

Ana Oncina Mico
Sustainable Energy Engineering
KTH Royal Institute of Technology

TRITA-ITM-EX 2024:451

Place for Project

Västerås, Sweden

Examiner

Björn Laumert
Stockholm
KTH Royal Institute of Technology

KTH Supervisor

Silvia Trevisan
Stockholm
KTH Royal Institute of Technology

UPV Supervisor

Emilio Jose Sarabia Escriva
Valencia
UPV Universitat Politècnica de València

ABB Supervisor

Moksadur Rahman
Västerås
ABB

Contents

1 Introduction **1**

2 Theoretical Background **3**

2.1 The Steel Industry 3
2.2 Mini-mill 5
2.3 Challenges in Traditional Steel Production 12
2.4 Technology Innovations towards Green Steel 13
2.5 Literature Review Summary 19

3 The Work **20**

3.1 Electric Arc Furnace Model 21
3.2 Reheating Furnace 33
3.3 Preheating Furnace 39

4 Results **41**

4.1 EAF 41
4.2 Reheating Furnace 47
4.3 Preheating EAF 51
4.4 Economics 55

5 Conclusions **64**

5.1 Answer to the research questions 64
5.2 Future Work 66
5.3 Summary 67

References **68**

1 Introduction

Steel is a critical component of modern society, with a diverse range of applications. Steel is employed in a multitude of applications, including construction and mobility. Furthermore, steel is playing an increasingly important role in the energy transition, with applications in the construction of wind turbines, solar panels, dams, and electric vehicles.

Over the past 50 years, there has been a threefold increase in demand for steel, and this trend is set to continue as economies develop [1]. However, the production of steel represents a significant environmental challenge for future industrial development. At present, steel production is responsible for 8% of global CO_2 emissions [1]. In consideration of the anticipated increase in steel production, it is necessary to implement environmentally responsible practices in steel manufacturing.

The European Union has set an ambitious target of reducing 55% of its emissions by 2030 and achieving a 100% carbon-free continent by 2050, in line with the goals set out in the European Green Deal [2]. The IEA has stated that the steel industry is not on course to achieve these goals [1].

There are numerous pathways for steel production, which is currently a highly carbon-intensive process. Steel production is composed of four production sections, those being raw material production, iron-making, steel-making, and post-processing. Most of CO_2 emissions in the steel industry are derived from the iron-making process, representing 70% of the industry's total CO_2 emissions [3]. As shown in Figure 2.1, the emission intensities associated with steel manufacturing as a whole range from 2.2 to 0.3 tCO_2e/t of steel.

To address the challenges associated with traditional steel production, the development of green steel is underway. Green steel refers to the production of steel with a significantly reduced carbon footprint, achieved through environmentally sustainable practices. The steel industry is incorporating renewable energy sources and utilizing hydrogen as a reducing agent to minimize the reliance on fossil fuels throughout the production process. Currently, the production of green steel is limited and remains a focus of ongoing research.

However, it is projected that production capacity will expand in the coming years [1].

The iron-making process is the primary source of emissions in steel production, which is why green steel initiatives have largely focused on this stage. To meet the objectives of this thesis, subsequent processes in steel manufacturing have been integrated into the energy model. This model evaluates the decarbonization potential of various electrification technologies and assesses their economic viability for adoption in the industry. Nevertheless, the literature review will encompass the full spectrum of potential decarbonization strategies for steel manufacturing. By evaluating the entire steel production process, this review aims to identify potential synergies between different stages, thereby facilitating a more comprehensive and effective approach to decarbonization. This approach will also enable the identification of a broader range of applicable technologies for mini-mill operations. Additionally, this study will explore potential solutions for heat integration across various process steps, with the ultimate goal of achieving a net-zero steel-making process.

2 Theoretical Background

The objective of this chapter is to provide a critical analysis of the existing literature and technological innovations to identify the complex dimensions of green steel. It examines the various environmental factors driving the transition to sustainable steel production and the technological advances that are transforming the industry.

2.1 The Steel Industry

The initial step is to examine the present-day production of steel. The industry produces steel through two methods: primary steel production, which involves the production of steel from iron ore, and secondary steel production, which consists of the production of steel from scrap steel, as steel is a highly recyclable material. In Europe, the secondary steel production route accounts for 40% of the total steel produced [4]. Figure 2.1 shows the two steel production routes together with related emissions at each production step. To gain a more comprehensive understanding of the emissions associated with each production route, Table 2.1 presents a summary of the energy consumption and emissions for the three most prevalent production pathways.

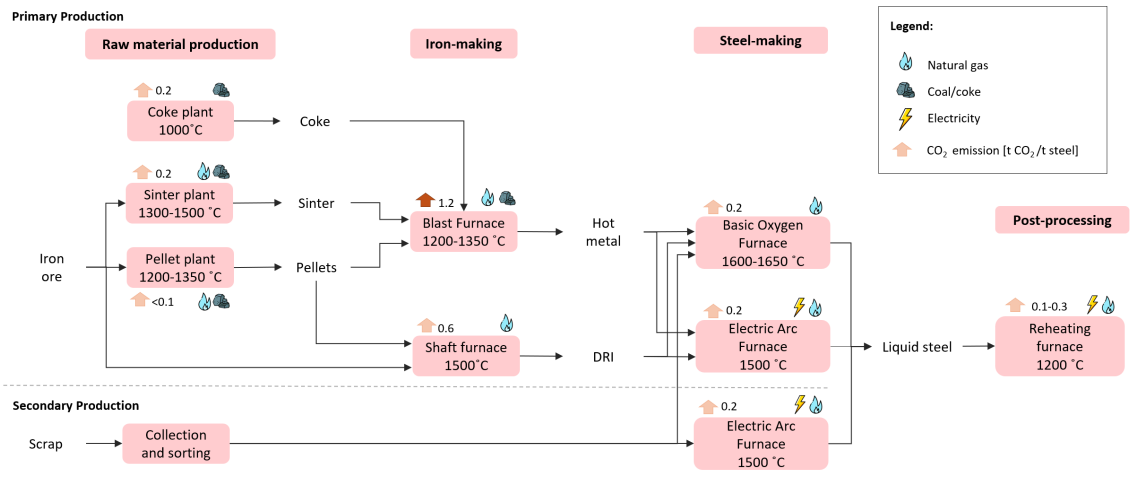

Figure 2.1: Steel production routes and its related emissions[1] [4]

As shown in Table 2.1, BF-BOF route, which involves iron-making in the Blast Furnace (BF) and steel-making in the Basic Oxygen Furnace (BOF), is significantly more energy and emission-intensive than the scrap-based EAF process for steel-

	BF-BOF	DRI-EAF	Scrap-EAF
Energy intensity [MWh/t steel]	5.94	4.75	0.58
CO_2 emissions [t CO_2/t steel]	2.2	1.4	0.3

Table 2.1: Energy Intensity & Emissions [1]

making. This is due to the fact that the Blast Furnace process requires the use of large amounts of coke and coal to reduce the mined iron ore prior to further processing it into steel, which is primarily done to increase the steel yield of the entire steel-making route. Moreover, the production of coke is an extremely energy-intensive process. The coke oven heats coking coal at temperatures around 1000 °C in the absence of air, requiring 1.8 MWh/t coke [4]. The blast furnace is also fed with sinter and pellets, which require preprocessing at temperatures around 1000 °C and requires 350 kWh/t hot metal [4].

Once the sinter or pellets have been charged into the Blast Furnace, hot air and pulverized coal are blown from the bottom, forming reducing gases from coke. These gases then undergo chemical reactions with iron ore, resulting in the production of hot metal. The process demands temperatures in the range of 1400°C and consumes approximately 3500 kWh/tn hot metal in the form of heat [4]. The hot metal produced by the blast furnace is then charged into the BOF. It is feasible to introduce scrap steel into the BOF, provided that the total metallic charge does not exceed 30% [4]. Following this, the hot steel is cast into various intermediary products through hot and cold rolling in downstream processes.

Waste gases resulting from these processes (production of coke, blast furnace, and blast oxygen furnace) are employed to recuperate energy within the system or to generate electricity.

In the secondary steel manufacturing process, steel scrap is melted in an Electric Arc Furnace (EAF) at temperatures of up to 1600 °C to produce liquid steel [4]l. While electricity is the primary energy input, natural gas, and chemical reactions account for 40% of the total energy input [4]. A small amount of carbon is still required in this furnace in order to foam the slag and improve the energy transfer between the arc and the melt, as well as for the final carbon content in the steel. This process requires energy only for the remelting of the scrap and

the addition of additives, resulting in much lower energy consumption and fewer process steps.

The second primary route of steel manufacturing shown in Table 2.1, combines the two methods mentioned previously. In this process, iron ore is mined and converted to Direct Reduced Iron (DRI), which is then fed into an Electric Arc Furnace. DRI is produced by feeding the iron ore into a shaft furnace and using natural gas as a reducing agent to reduce the iron oxide in the iron ore. The steel-making process has shifted from the Basic Oxygen Furnace, which required significant coal and coke input, to the Electric Arc Furnace, resulting in reduced emissions.

Regardless of the steel-making method employed, the steel slabs are transferred to a reheating furnace, which represents a significant source of energy consumption during the rolling and finishing stages. Consequently, the energy consumed and associated costs in this process stage are significant [5]. The furnace is typically fueled by natural gas and is used to reheat steel slabs from either room temperature or 800°C, which is dependent on the integration of the rolling mill with the steel-making process. The temperature of the steel slabs rises up to 1200 °C [6]. At this stage, the slabs have reached an adequate temperature for hot rolling. Following this step, an annealing process may be employed for further product finishing, which is dependent on the product's requirements [7].

2.2 Mini-mill

After an overview of the steel industry, this section provides a more detailed explanation of the mini-mill process, which will be the focus of the electrification option studies.

Figure 2.2 illustrates the functioning of a conventional mini-mill process. The process begins with the Electrical Arc Furnace, which melts the fed metal. The melt is then fed into a ladle to decarbonize and desulphurize the melt. The resulting steel is either directly fed into the reheating furnace at a temperature of 800 °C or it produces metal slabs that are stored and then fed into the reheating furnace at room temperature. These slabs are heated up to 1250 °C to then be hot rolled.

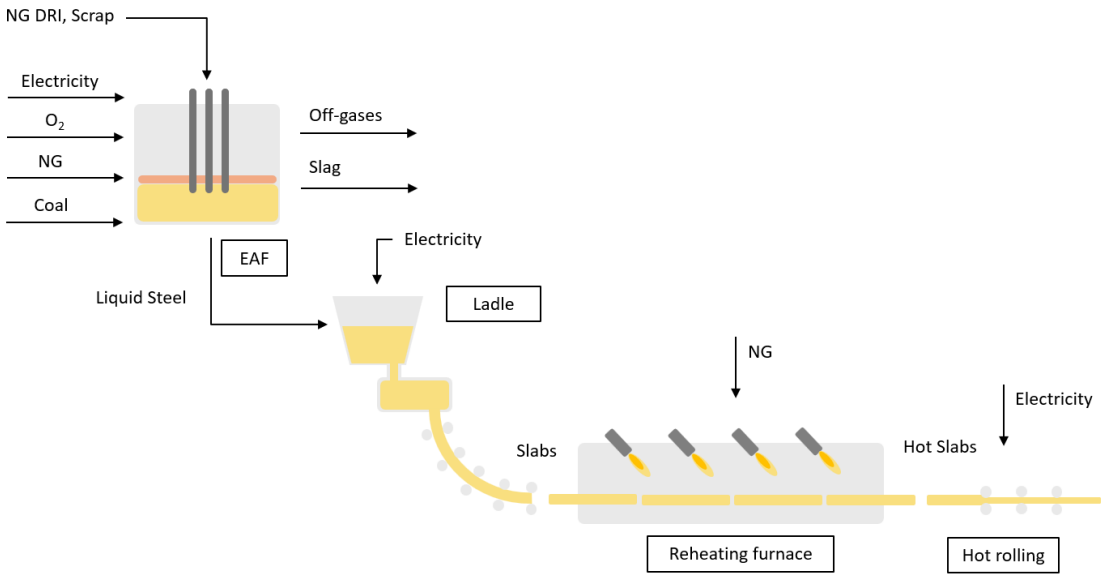

Figure 2.2: Mini-mill process

2.2.1 Electric Arc Furnace

The Electric Arc Furnace currently produces steel using 60% of its total energy from electricity, with the remaining 40% derived from diverse chemical reactions and natural gas combustion within the furnace [8]. Over time, the process efficiency and productivity have improved, in part due to technological innovations such as increased oxygen, carbon, foaming slag, and post-combustion of carbon monoxide.

The EAF process is a batch process that can be divided into four steps: charging with one or more scrap baskets, meltdown of the scrap, heating and refining, and finally tapping. At the beginning of the melt, the electrodes are bored down into the scrap pile with reduced power to prevent electrode breakages. When the electrodes reach the melt surface, high power is applied to melt the scrap, which is now shielding the furnace walls and roof from the electric arcs. Oxyfuel burners, which utilize fuels such as natural gas or oil, are employed to facilitate homogeneous melting in the cold spots of the furnace, thereby increasing productivity. The efficiency of burners is inversely related to the temperature within the furnace. Consequently, burners are not employed to the same extent at the end of the process when temperatures are considerably higher. At this stage, oxygen is introduced into the furnace, where it reacts with various components

of the melt, forming slag. These oxidation reactions are exothermic, releasing energy into the furnace, which contributes to the energy and reduces the amount of electricity required. The different chemical reactions are shown in the equations below.

$$Fe + \frac{1}{2}O_2 \rightarrow FeO, \quad \Delta H_r = -1.3\frac{kWh}{kg_{Fe}} \tag{1}$$

$$Si + O_2 \rightarrow SiO_2, \quad \Delta H_r = -8.94\frac{kWh}{kg_{Si}} \tag{2}$$

$$Mn + \frac{1}{2}O_2 \rightarrow MnO, \quad \Delta H_r = -1.93\frac{kWh}{kg_{Mn}} \tag{3}$$

$$2Cr + \frac{3}{2}O_2 \rightarrow Cr_2O_3, \quad \Delta H_r = -3.05\frac{kWh}{kg_{Cr}} \tag{4}$$

$$2Al + \frac{3}{2}O_2 \rightarrow Al_2O_3, \quad \Delta H_r = -5.29\frac{kWh}{kg_{Al}} \tag{5}$$

$$2P + \frac{5}{2}O_2 \rightarrow P_2O_5, \quad \Delta H_r = -5.54\frac{kWh}{kg_{P}} \tag{6}$$

Once the molten charge has reached a sufficient level of melting, the arcs are no longer shielded from the scrap. A second purpose of the oxygen lance is to produce foamy slag, which serves to shield the electric arcs and enhance the transfer of energy between the arc and melt. This foamy slag is acquired through the combination of oxygen lancing and injection carbon. The formation of carbon monoxide bubbles is a consequence of the initial oxidation of iron to iron oxide and subsequent reduction with carbon injection, which is followed by the return of iron to its original state.

$$Fe + \frac{1}{2}O_2 \rightarrow FeO \quad \Delta H_r = -1.32\frac{kWh}{kg_{Fe}} \tag{7}$$

$$FeO + CO_2 \rightarrow Fe + CO_2 \quad \Delta H_r = -17.47\frac{KJ}{mol} \tag{8}$$

$$CO_2 + C \rightarrow 2CO \quad \Delta H_r = +165.52\frac{KJ}{mol} \tag{9}$$

$$FeO + C \rightarrow Fe + CO \quad \Delta H_r = +148.05\frac{KJ}{mol}; \Delta H_r = +3.43\frac{kWh}{kg_C} \tag{10}$$

It is of importance to note that the reduction reaction occurring in formula 10 is a combination of reactions 8 & 9 that result in an endothermic reaction, whereby energy is absorbed from the system. However, when considering the reaction represented by formulas 7 & 10, it can be considered that it results in the direct production of carbon monoxide and ultimately an exothermic reaction overall.

$$C + \frac{1}{2}O_2 \rightarrow CO \quad \Delta H_r = -2.66\frac{kWh}{kg_C} \tag{11}$$

Nevertheless, as the reduction of iron oxide is an endothermic reaction, it is of the utmost importance to pay close attention when determining the quantities of oxygen and carbon to be introduced into the furnace. An excess of oxygen will result in a decrease in electrical consumption due to an exothermic reaction. However, this will also result in a reduction in the yield of steel, as iron is left in the slag as iron oxide. Conversely, if excess carbon is introduced, the reaction will consume more oxygen, potentially increasing steel yield but also raising electrical consumption.

Throughout the process, injected carbon and oxygen also react to form carbon monoxide, releasing energy in the system. Another energy contributor is electrode decomposition, which dissolves carbon in the melt which then reacts with oxygen, forming carbon monoxide and carbon dioxide. The electric arc furnace employs three electrodes to transform electrical energy into thermal energy via a plasma arc. As the electrodes are used, they gradually degrade. Given that the electrode is composed of 99% carbon, its decomposition plays a role in the electric arc furnace energy and mass model [8][9]. On the one hand, the carbon that is dissolved in the melt oxidizes to carbon dioxide with a high energy transfer efficiency to the melt, around 100%. On the other hand, this carbon dioxide that has been generated contributes to the off-gases of the system and therefore also contributes to the emissions of such.

Moreover, the extent of decomposition of the electrodes will depend on the electric intensity required in the system. The greater the electrical intensity, the more rapid the degradation is. This phenomenon is typically observed when low-carbon metals are introduced into the furnace [10]. Further oxygen injection or infiltered air is added to the furnace to achieve post-combustion energy from the chemical reaction.

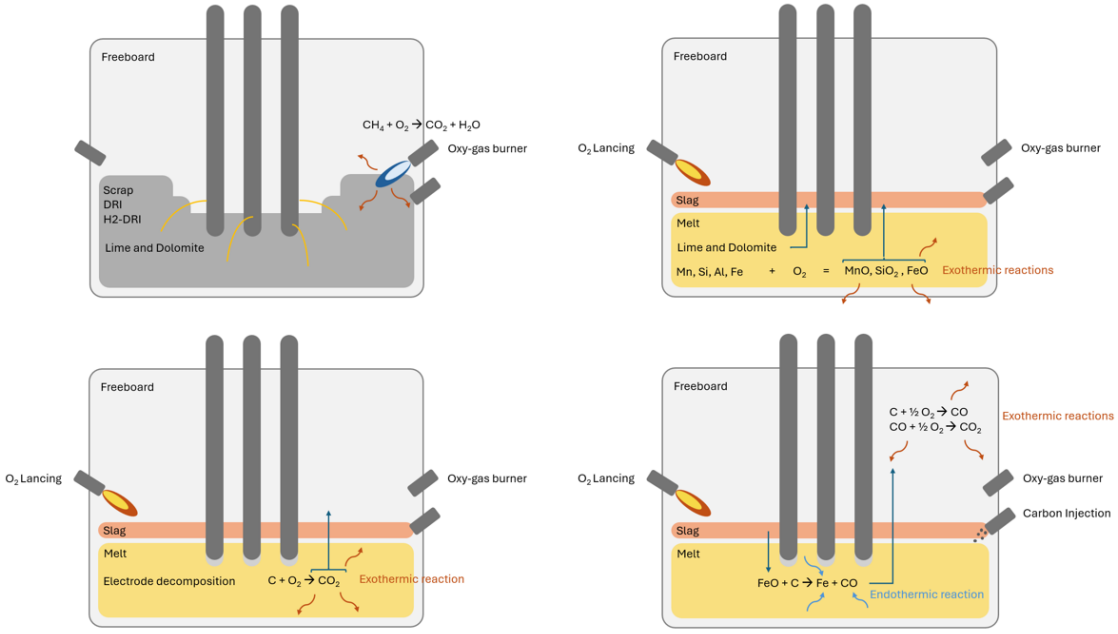

Figure 2.3: Stages in the Electric Arc Furnace

The schematic overview presented in the image above illustrates the various stages of operation within an Electric Arc Furnace. This visual representation is designed to facilitate comprehension for the reader.

2.2.2 Feeding the Electric Arc Furnace with different input metals

Although the preceding section has presented the behavior of the Electric Arc Furnace from the perspective of scrap feeding alone, this study will also analyze the distinct metal inputs of DRI and Hydrogen DRI.

As previously introduced, Direct Reduced Iron (DRI) is defined as iron ore that has undergone a reduction process utilizing natural gas as the reducing agent in a shaft furnace. In this process, not only is the iron oxide in iron ore reduced in order to achieve a higher yield of steel, but the material is also carburized.

This carburization occurs in two different ways. The first is carburization by free carbon in the material, and the second is based on the formation of cementite (Fe_3C). The formation of these two distinct components has a significant impact on the functioning of the Electric Arc Furnace.

In contrast with the scrap heating process utilized in the EAF, in which scrap is charged at the initial stage of the melting process, known as batch charging, the charging of DRI is conducted through a continuous feeding method. This is regardless of whether the DRI in question is natural gas-based or hydrogen-based. The mentioned continuous feeding method is executed via the fifth hole of the EAF, which serves as a feed port throughout the melting process [11]. To address the challenges associated with the melting of DRI, the continuous charging process is necessary to prevent the formation of metal icebergs within the melt in the EAF [12]. Moreover, this charging method affects the behavior of the DRI in the energy and mass balance of the furnace [11].

DRI generally presents a composition of carbon comprising 20% free carbon and 80% carbon in the form of cementite (Fe_3C)[13]. As DRI is charged throughout the melting process, the free carbon of the DRI is directly combusted in the freeboard of the Electric Arc Furnace, thus not reaching the melt. This results in some heating energy being transferred to the system, but it does not participate in the chemical reactions of the melt[11, 14]. On the other hand, cementite (Fe_3C) must first dissociate in order for the carbon to interact in the chemical processes [11, 13]. When cementite is deposited in the furnace, it begins to heat until it reaches its solidification temperature of 1500 K, at which point it will begin to dissociate[11]. This occurs when the DRI pellet has already reached the liquid bath. The dissociation process itself is an exothermic reaction, therefore some energy will be released into the liquid bath. Once it has dissociated, this carbon will then react with oxygen to generate carbon monoxide bubbles, which will increase the heat transfer efficiency from the arc to the melt. These bubbles are smaller and more stable than those generated by injected carbon. Furthermore, these CO bubbles will react with the iron oxide in the slag, contributing to the reduction reaction and increasing the steel yield [11, 13].

The primary distinction between natural gas-based DRI and hydrogen-based DRI

lies in the absence of carbon in hydrogen-based DRI [15]. This lack of carbon in the DRI presents certain challenges. In the absence of additional carbon injected into the EAF to reduce the iron oxide in the melt, a considerable amount of iron will be lost in the slag [16, 17]. Furthermore, the heat transfer efficiency of injected carbon is considerably lower than that of in-situ carbon in the metal. Consequently, additional electrical energy will be required within the system[16]. This study aims to quantify the associated energy requirements and CO_2 emissions from this process stage, given the projected growth in H2 DRI as an input metal in EAF in the coming years. This is a critical consideration for the development of environmentally sustainable steel production.

2.2.3 Ladle Furnace

The ladle furnace is a critical component in the steel production process, enabling the final adjustment of temperature and composition of molten steel in a cost-effective manner. This process occurs in a reduced atmosphere with argon stirring and utilizes a submerged arc heating system. This allows preceding processes, such as the electric arc furnace, to focus on rapid heating, with subsequent steel composition adjustments made in the ladle furnace.

Following the ladle furnace, the molten steel is continuously cast in various forms, including slabs, billets, and blooms. Molten steel is poured into open-bottomed water-cooled molds, where the outer shell solidifies as the steel passes through the mold.

In the context of this project, the ladle furnace will not be evaluated, as it does not represent a significant emission source within the context of the mini-mill.

2.2.4 Reheating Furnace and hot rolling

The reheating furnace is a critical process step in downstream steel-making operations. Heating the steel to 1200°C induces recrystallization, thereby reducing the mechanical energy required for steel forming by a factor of 8 to 10 [6]. To achieve this temperature, the industry predominantly employs natural gas-fired furnaces for heating steel slabs.

In some cases, furnaces utilize waste heat from coke ovens and blast furnaces, or the heat from the same process is used to preheat the air entering the furnace.

2.3 Challenges in Traditional Steel Production

As previously stated, the steel production process is heavily reliant on fossil fuels, such as coal and natural gas. In Figure 2.1 the various emissions associated with steel production are shown. It is notable that the primary steel production route produces considerably more emissions than the secondary steel production route, particularly in terms of emission intensity associated with the blast furnace. However, the steel industry cannot rely solely on producing scrap-based EAF steel to meet current demand, as scrap is not widely available due to the long service life of steel products [18]. Figure 2.4 shows that 100% Scrapped-based steel-making is not foreseen in future scenarios of the European Union.

As previously indicated, the steel production process is heavily dependent on fossil fuels, such as coal and natural gas. Figure 2.1 illustrates the various emissions associated with steel production. It is noteworthy that the primary steel production route generates significantly higher emissions compared to the secondary steel production route, particularly in terms of emission intensity associated with the Blast Furnace. However, the steel industry cannot rely solely on producing secondary steel (Scrap-EAF) to meet current demand, as scrap availability is limited due to the long service life of steel products [18]. Figure 2.4 demonstrates that 100% secondary steel production is not anticipated in future scenarios for the European Union.

Technological advancements are necessary for producing cleaner primary steel [19]. Research indicates that emission reduction potential in the traditional steel sector is limited, with established steel production routes collectively abating only approximately 25-40% of average CO_2 emissions per ton of crude steel produced [20]. Additionally, in the European context, steel plants are already highly integrated, offering minimal opportunities for further energy integration. Therefore, achieving further reductions necessitates the development and implementation of breakthrough technologies [4].

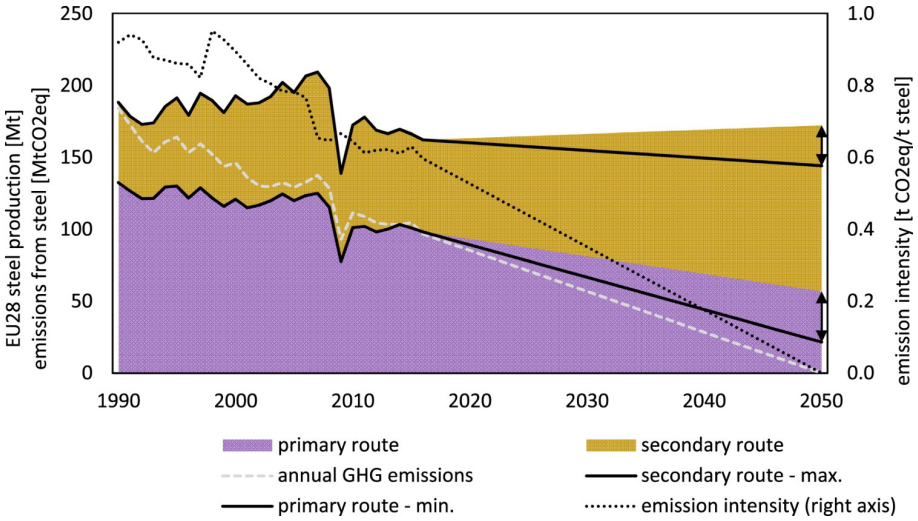

Figure 2.4: Steel production EU [19]

2.4 Technology Innovations towards Green Steel

As explained in section 2.3, the steel industry must take significant steps to transform the production process into a more sustainable one. This section examines the main technologies and strategies available to achieve green steel and is divided into four subsections, depending on the method used to reduce emissions.

2.4.1 Carbon Capture Technology

This section on carbon capture encompasses both carbon capture and storage (CCS) and carbon capture and utilization (CCU). These technologies are crucial as many blast furnaces will remain operational in the coming years, and they can significantly reduce emissions. CCS is essential for the industry's decarbonization, offering a cost-effective and practical method to mitigate process emissions. It is a pivotal technology that supports the continued operation of the existing industry while facilitating its decarbonization in line with the Paris Agreement objectives. Although CCS is currently viewed as a promising approach for emission reduction, it can decrease the overall efficiency of a steel plant due to the high energy consumption required for capture processes [21]. Therefore, further innovation is necessary. An alternative solution is carbon capture and utilization (CCU), which does not require large quantities of hydrogen to upgrade off-gas to higher-value gases and can be considered a waste mitigation technology.

The primary objective of CCS is to facilitate the continued operation of existing BF-BOF facilities while new, lower-emission plants are developed. However, the BF-BOF route has multiple CO_2 emission points, and the recirculation of off-gases within the plant further complicates this issue. Among the three waste gases produced in a BF-BOF steel plant (Blast Furnace, Coke Oven, and Basic Oxygen Furnace gases), Blast Furnace gas has the highest CO_2 emissions and the lowest heating value. Consequently, most projects aiming to integrate CCS and CCU technologies focus on applying them to the Blast Furnace alone [22].

Current CCUS projects in the steel industry successfully capture between 19% and 26% of emissions [23]. According to the latest IEA projections, the decarbonization of the steel industry is more likely to progress than the development of CCUS based on current trends.

2.4.2 Hydrogen as a reducing agent

This section will examine various technologies that utilize hydrogen as a reducing agent. Given that iron reduction predominantly occurs during the iron-making process, the subsequent section will primarily focus on this aspect of steel production.

H2-DRI

The iron-making process contributes approximately 70% of the total emissions [3]. However, improving process efficiency and reducing emissions has proven difficult with the conventional Blast Furnace iron-making process. Direct hydrogen reduction is considered the most promising technology for carbon-free steel-making.

Several projects are currently underway to produce Hydrogen Direct Reduced Iron (H2-DRI). This process involves replacing natural gas with hydrogen as the reducing agent in the shaft furnace. Some projects are gradually replacing natural gas with hydrogen in existing shaft furnaces, such as in Germany, while others, such as pilot projects in Sweden, have redesigned the shaft furnace to use hydrogen exclusively. Examples of both methods are listed in Table 2.2, which details current projects and their respective hydrogen content.

Company	Country	% H2 SF
HYL ENERGIRON	Italy	0-100
MIDREX	Germany	30-100
SALCOS	Germany	100
HYBRIT	Sweden	100
H2 Green Steel	Sweden	100

Table 2.2: H2-DRI ongonig proyects [15]

This technology replaces CO_2 emissions in the shaft furnace with water vapor, offering significant opportunities for emissions reduction. However, the resulting DRI lacks carbon content and has a higher iron oxide content, which requires a larger amount of carbon in the Electric Arc Furnace. Nevertheless, the total amount of carbon used in both processes is still lower than in the process using natural gas based DRI. [15]

In a similar approach to hydrogen reduction, trials have been conducted in German blast furnaces to gradually reduce the quantity of coal used by substituting it with hydrogen. These tests have generated a substantial amount of data, which will aid in the optimal utilization of hydrogen. However, further work is currently in progress [24].

Smelting reduction H2 plasma

Hydrogen Plasma Smelting Reduction (HPSR) is a key technology for achieving green steel production. In this process, a plasma arc is generated between an electrode (cathode) and the molten bath (anode). Iron ore fines, hydrogen and, argon are introduced into the reduction zone via a hollow electrode. The charged ore is melted in the flow and reduced to metallic iron with ionized hydrogen producing steam as a by-product [25]. Recent studies are exploring the impact of using DRI in the process as an input, thereby reducing the overall use of hydrogen [26].

At the industry level, Voestalpine is the only company involved in a development project in which HPSR technology is being considered. This project, called SuSteel, has a plant in Donawitz, Austria, which started operations in 2021 [27].

2.4.3 Hydrogen as a heat source

The use of hydrogen can be extended not only to the iron and steel-making process but also to ancillary processes such as reheating furnaces. As explained in section 2.1, these also involve a significant amount of CO_2 emissions from burning natural gas. However, hydrogen could also be used for this process step, representing an opportunity to reduce emissions. This has already been achieved by the Swedish company Ovako in its rolling mills in 2023. To achieve this, Ovako owns the largest electrolysis plant in Sweden, with a rated capacity of 20 MW, capable of producing 3,880 cubic meters of hydrogen per hour [28].

2.4.4 Electrification of the iron and steel- making process

An innovative technology based on the electrolysis principle is currently being developed, which employs electricity to reduce iron ore into iron. The process involves passing an electric current through iron ore in an electrolyte, which leads to the formation of positively charged iron ore ions that migrate towards the negatively charged cathode, where they are reduced to iron. Conversely, negatively charged oxygen ions move to the anode and are released from the solution. The electrolysis process produces no direct CO_2 emissions, potentially making it a carbon-neutral technology if the electricity used to power the system is from renewable sources [4, 29].

Although, as with hydrogen plasma reduction, iron ore electrolysis is not a mature technology with a TLR 4 [1], two electrolysis routes are currently under investigation. One is low-temperature alkaline iron electrolysis working at a temperature of 100 °C, a process that would replace the iron-making process, also known as electrowinning. The steel-making process would still be required. Additionally, high-temperature Molten Oxide Electrolysis (MOE) has been proposed as a potential technology for the production of liquid steel. This process operates at temperatures of 1600 °C and would eliminate the need for multiple steps in the steel manufacturing process [29, 30].

The most significant limitations of these technologies are, on the one hand, the lack of suitable anode material capable of withstanding the challenging conditions in the cell for MOE process. Furthermore, the inconsistency in the obtained

iron is a result of the difficulty in the electrowinning process. Therefore, further clarification and control of the reduction process of Fe_2O_3 are essential for the technology to be further developed.

2.4.5 Electrification of reheating furnace

The direct electrification of industrial furnaces could represent a significant step towards decarbonizing iron and steel plants. There are multiple potential options for electrifying the reheating furnace. The following paragraphs will examine three key technologies: electrical heating, plasma torch, and induction heating.

Resistive heating

Electrical heating represents a viable alternative for CO_2-neutral process heat generation in continuous reheating furnaces, particularly in consideration of the CO_2 emission factors. Electrical heating elements are available on the market for smaller installations. However, to reheat steel in high-capacity continuous reheating furnaces, these elements are not yet capable of achieving the necessary surface load by the current state of the industry's technical knowledge [6].

Induction heating

Induction heating is a process that utilizes the heat generated by currents induced within a conducting body that is exposed to an alternating magnetic field produced by an AC current flowing in an inductor coil. The primary advantages of this process are the transmission of electromagnetic energy from the inductor to the workpiece without direct contact and the ability to rapidly and selectively heat specific regions of the workpiece [31].

The most significant industrial applications of induction heating include the melting of metals, the heating of metals prior to hot working, such as rolling, forging, and stamping, and finally, heat treating, with particular attention to surface hardening at medium and high frequencies.

Plasma

As an alternative, plasma heating torches have been shown t be an effective

solution [32]. Plasma heating torches offer several key advantages, including a high temperature in the plasma jet, a high energy density for the plasma, controlled process chemistry, small installation sizes, and rapid start-up and shutdown features. It is important to consider the implications of replacing conventional gas burners with plasma torches. It is therefore necessary to consider parameters such as sufficient temperature, no effect on steel quality, and equal or even higher furnace efficiency. It is therefore important to select an appropriate plasma carrier gas and other operating parameters to achieve high efficiency and low emission levels in plasma heated furnaces [32].

2.4.6 Bioenergy technology

There has been a significant increase in interest regarding the utilization of renewable biomass as a heating source and as a substitute for fossil fuels within the steel industry. This approach has the potential to substantially reduce carbon dioxide emissions associated with steel production processes, thereby offering considerable environmental benefits. However, the adoption of biomass in the steel industry remains constrained by strong competition from fossil fuels.

Despite extensive research conducted independently in these areas, there is a notable lack of integration between them. From both economic and technical perspectives, the partial substitution of fossil fuels such as coal and coke with renewable biomass products in iron-making processes represents one of the few viable options that could be implemented in the near future [33]. It is crucial to recognize the distinctive properties of biomass, which include renewability, carbon neutrality, low sulfur content, and low ash content.

The interactions between the biomass-based and steel production sectors are crucial for enhancing the overall performance, efficiency, and sustainability of these industries. Technological advancements are underway, as exemplified by ArcelorMittal's "Torero" project in Belgium [34]. This initiative aims to reduce the volume of fossil coal used in blast furnaces by replacing it with a bio-coal substitute.

Further research has been conducted on the implementation of biomass in EAFs, including the use of biochar to substitute coal and bio-gas to substitute natural

gas. This study, conducted by the European project GreenEAF, demonstrated the technical feasibility of these approaches [35]. The economic evaluation highlighted the sustainability of replacing coal with char from biomass, along with environmental benefits due to reduced CO_2 emissions.

2.5 Literature Review Summary

Following an extensive review of the literature regarding the technologies that can drive forward Green Steel production, the following table has been prepared to summarize the various technologies that apply to the different process steps.

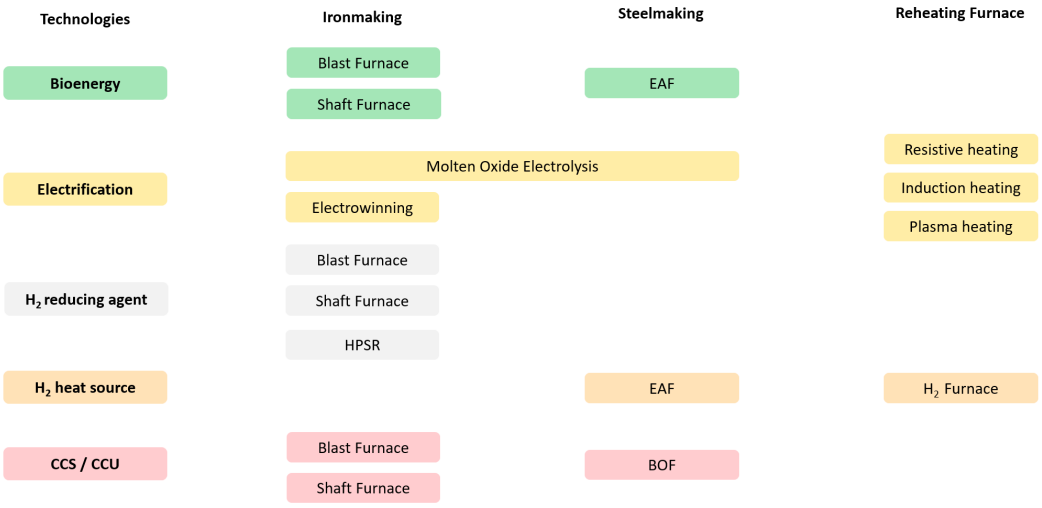

Figure 2.5: Technology advancements driving 'green steel' in sustainable production.

A review of the literature reveals that a considerable proportion of attention within the industry is focused on the decarbonization of the iron-making segment with all types of different approaches as illustrated in Figure 2.5. However, a gap has been identified concerning the decarbonization of the mini-mill section. This thesis aims to address this gap by investigating the integration of electrification technologies in mini-mills to decarbonize the industry.

3 The Work

As established in Section 2.5, a gap has been identified in the decarbonization potential of mini-mills. To address this, a selected group of decarbonization technologies, as studied in the literature review, are modeled and contrasted with state-of-the-art technologies. These models will be explained in the present chapter, enabling an evaluation of the energy intensity requirements and emissions reduction potential of the selected solutions.

As established in Section 2.5, a gap has been identified in the decarbonization potential of mini-mills. To address this, a selected group of decarbonization technologies, as reviewed in the literature, are modeled and compared with state-of-the-art technologies. The present chapter will elucidate these models, facilitating an evaluation of the energy intensity requirements and emissions reduction potential of the proposed solutions.

The study assesses the performance of various preheating technologies to be utilized prior to scrap entering the Electric Arc Furnace. Subsequently, the efficacy of several distinct heat sources for this preheating process will be evaluated and contrasted with the energy savings derived from the EAF as a result of preheating. Furthermore, the work will investigate the influence of varying metal inputs on the energy balance of the Electric Arc Furnace, given that previous research indicates that the transition from hydrogen-derived direct reduced iron (H_2-DRI) has the potential to increase the carbon intensity of the EAF, making it more carbon-intensive than the use of natural gas-based DRI. In addition, the reheating furnace following the EAF and preceding the hot rolling process will be investigated with various electrification technologies, including plasma torches and indirect electrification methods, such as hydrogen combustion. Finally, an economic analysis will be conducted taking into consideration future trends such as carbon pricing as well as natural gas and electricity prices. These different studies are shown in Figure 3.1.

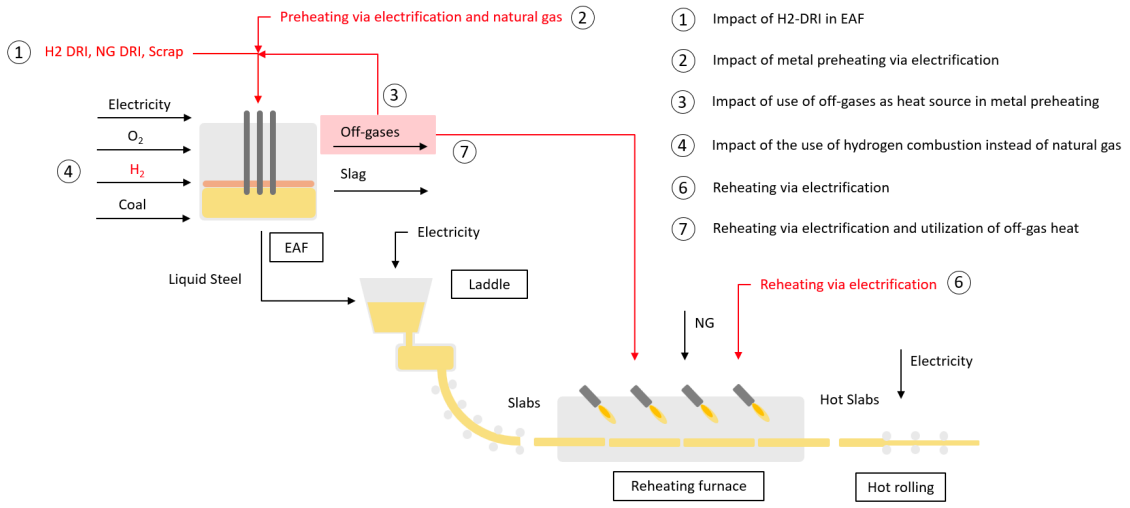

Figure 3.1: Decarbonazation Studies

3.1 Electric Arc Furnace Model

This study presents a detailed model of the Electric Arc Furnace (EAF), a complex system with many interconnected components. The model examines four key functions in depth: Oxygen Lancing, Injection Coal, Electrode Decomposition, and Oxy-Gas Burner. The complexity of the EAF means that the study's results and conclusions are significantly influenced by the type of metal input used.

To understand the energy dynamics within the EAF, the system relies on five primary energy inputs: oxygen lancing, carbon injection, electrode decomposition, oxy-gas burner, and electricity. The ratios of these inputs vary based on the metal charged into the furnace. Formulas 12, 13, and 14 represent the energy balance of the entire EAF system (system boundary 1), demonstrating that energy input equals energy output, indicating a balanced system. Figure 3.2 illustrates the two system boundaries used in the model.

$$Q_{total} = Q_{in} = Q_{out} \tag{12}$$

$$Q_{in} = Q_{electric} + Q_{oxygen\ lancing} + Q_{carbon\ injection} + Q_{oxy-gas\ burners} + Q_{electrodedecompositon} \tag{13}$$

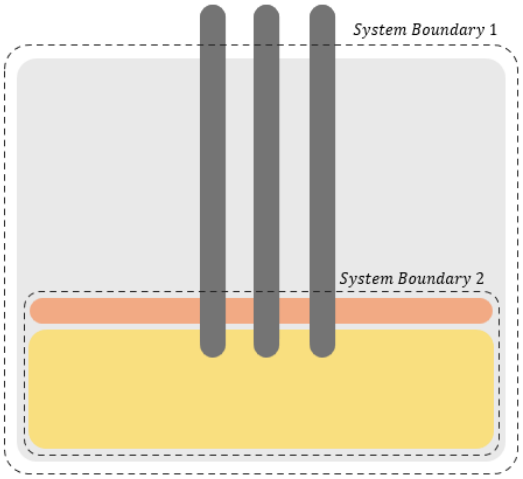

Figure 3.2: System Boundaries EAF

$$Q_{out} = Q_{steel} + Q_{slag} + Q_{off-gas} + Q_{shell} \tag{14}$$

The energy output parameters consist of four components: steel, slag, off-gas, and shell. The energy transferred to both the steel and the slag is defined as the energy of the melt. The melt exits the furnace at a temperature of 1650 °C, and its energetic value is calculated as follows.

$$\Delta H_{melt} = Q_{steel} + Q_{slag} \tag{15}$$

$$Q_{steel} = m_{steel} \times \int_{T_{ref}}^{T_{steel_{out}}} c_{p_{steel}}(T)\, dT \tag{16}$$

$$Q_{slag} = m_{slag} \times \int_{T_{ref}}^{T_{slagout}} c_{p_{slag}}(T)\, dT \tag{17}$$

To calculate the specific enthalpy of both steel and slag, various heat capacities were evaluated according to the literature to ensure an accurate correlation between the energy outputs and the functioning of the EAF. According to the literature, the energy content of steel at the end of the EAF process is approximately 390 kWh/t steel [8, 36]. To provide a comprehensive and adaptable model for future use, the enthalpies of various steel types were

examined and can be integrated into the model. Figure 3.3 illustrates how the thermal properties of steel change with composition. Since the thermal properties of steel are highly dependent on its composition, material testing is essential for understanding its thermal behavior.

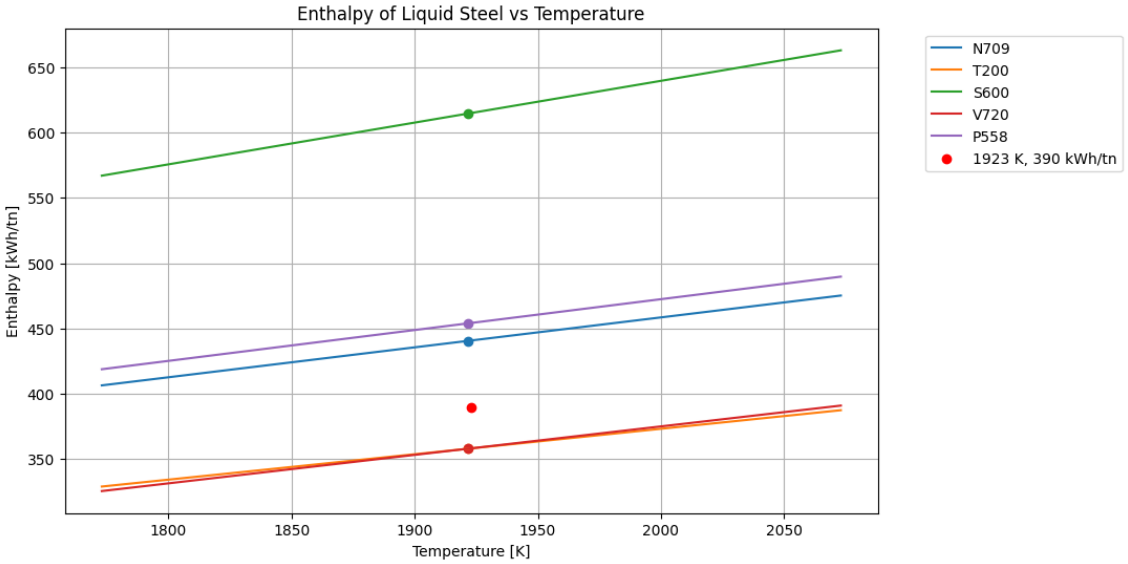

Figure 3.3: Specific Enthalpies of five different liquid steel alloys [37]

These specific enthalpies have been computed as follows:

$$y = a + bT \tag{18}$$

The table provides the parameters for the various steel types that are necessary for calculating the enthalpies at a specific temperature.

	a	b	Range T [K]
V720	-220	0.7852	1814<T<2550
S600	-0.06209	1.1514	1688<T<2400
N709	-0.02746	0.8254	1719<T<2600
P558	-0.03393	0.8505	1723<T<2500
T200	-58.8	0.7013	1719<T<2600

Table 3.1: Specific Enthalpy parameters for Liquid Steel [37]

The data used to calculate the heat content of the slag was derived from the enthalpy values presented in Figure 3.4. As observed, the crystallization temperature of the slag is reached at approximately 1200 °C. From the point (T = 1500 °C), it is assumed that the enthalpy of the slag continues to increase linearly, with the enthalpy at 1650 °C being extrapolated.

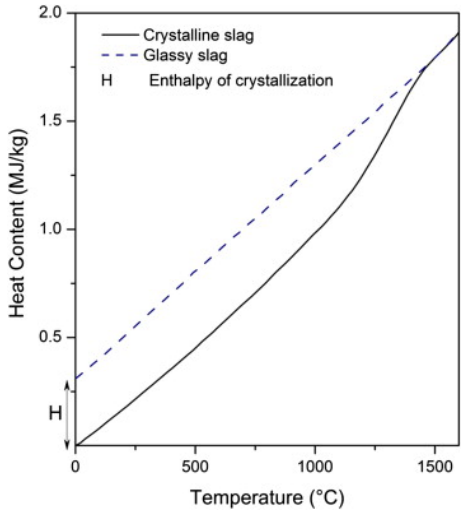

Figure 3.4: Heat Content of Slag

The objective of the energy transfer from the various energy sources within the furnace is to raise the temperature of the melt. To simplify the calculations, different efficiencies have been established for each energy input. These efficiencies represent the amount of energy that is effectively transferred to the melt. This corresponds to system boundary 2, as illustrated in Figure 3.2.

$$\Delta H_{melt} = Q_{steel} + Q_{slag} = \eta_{el} Q_{electric} + \eta_{ol} Q_{oxygen\ lancing} + \eta_{ci} Q_{carbon\ injection} + \eta_{bur} Q_{oxy\text{-}gas\ burners} + Q_{electrode\ decomposition} \quad (19)$$

Given that the left-hand side of equation 19 is known and that the right-hand side contains only one unknown, namely the energy input from electricity, the system can be resolved. This resolution allows us to proceed to the second part of the energy balance.

$$Q_{off-gas} + Q_{shell} = (1-\eta_{el})Q_{electric} + (1-\eta_{ol})Q_{oxygen\ lancing} + (1-\eta_{ci})Q_{carbon\ injection} + (1-\eta_{bur})Q_{oxy\text{-}gas\ burners} \quad (20)$$

In this instance, the unknown parameter is the heat of the off-gas. Consequently, the exit temperature of the off-gases will be determined by the following equation.

$$Q_{off-gas} = \sum_i m_i \times \int_{T_{ref}}^{T_{off-gas}} c_{p_i}(T)\, dT\,;\ i \quad \epsilon \quad off-gas \quad components \quad (21)$$

As illustrated in Equation 21, the off-gas is calculated as the sum of the enthalpies of its distinct components: nitrogen, oxygen, carbon monoxide, carbon dioxide, and water. Similar to the enthalpy of steel, several temperature-dependent calorific capacities have been employed in calculating the different enthalpies. The methodology used is shown in formula 22, and the specific parameters for each gas are presented in Tables 3.2, 3.3, 3.4, 3.5, and 3.6.

$$c_{p_i}(T) = A_i + B_i\frac{T}{1000} + C_i(\frac{T}{1000})^2 + D_i(\frac{T}{1000})^3 + E_i(\frac{T}{1000})^{-2} \quad (22)$$

with T[K] and Cp_i [J/molK]

Temperature [K]	**A**	**B**	**C**	**D**	**E**
100 < T <500	28.99	1.85	-9.65	16.64	0.00
500 < T < 2000	19.51	19.89	-8.60	1.37	0.53

Table 3.2: Parameters for calorific capacity of nitrogen [38]

Temperature [K]	**A**	**B**	**C**	**D**	**E**
100 < T <700	31.32	-20.24	57.87	-36.51	-0.01
700 < T < 2000	30.03	8.77	-3.99	0.79	-0.74

Table 3.3: Parameters for calorific capacity of oxygen [39]

Temperature [K]	A	B	C	D	E
298 < T <1300	25.57	6.10	4.05	-2.67	0.13
1300 < T < 6000	35.15	1.30	-0.21	0.01	-3.28

Table 3.4: Parameters for calorific capacity of carbon monoxide [40]

Temperature [K]	A	B	C	D	E
298 < T <1200	25.00	55.19	-33.69	7.95	-0.14
1200 < T < 6000	58.17	2.72	-0.49	0.04	-6.45

Table 3.5: Parameters for calorific capacity of carbon dioxide [41]

Temperature [K]	A	B	C	D	E
500 < T <1700	30.09	6.83	6.79	-2.53	0.082
1700 < T < 6000	41.96	8.62	-1.50	0.10	-11.16

Table 3.6: Parameters for calorific capacity of water vapor [42]

3.1.1 Metal Feeding

As previously outlined in section 2.2.2, the EAF is capable of processing various feedstock materials. For this thesis, three specific charge materials have been considered: scrap, Direct Reduced Iron (DRI), and hydrogen-based Direct Reduced Iron H_2-DRI. In the case of scrap, a detailed scrap receipt has been entered into the model, reflecting the common practice in mini-mills of using a mix of different scrap types.

The proportions of the various feedstock materials in the model are determined by three parameters: x_scrap, x_DRI, and x_H_2-DRI. The sum of these parameters must equal one to ensure the accurate calculation of the system. The compositions of the different materials have been provided by industry sources. A function has been developed to determine the final composition of the material mixture.

3.1.2 Oxy-gas burner

The incorporation of oxy-gas burners in the EAF facilitates more homogeneous melt heating compared to the use of electric arcs alone. Consequently, various mixing techniques are employed alongside oxy-gas burners, including the use of inert gases and magnetic fields to enhance the homogeneity of temperature within the melt. Oxy-gas burners are dedicated to the melting of metal, allowing for the substitution with hydrogen combustion.

The efficiency of oxy-gas burners in heating a material is dependent on the temperature of the material being heated, with the efficiency of heat transfer being inversely proportional to the temperature of the material. Therefore, these burners are utilized exclusively during the initial operational phase of the EAF. The overall efficiency of oxy-gas burners in an EAF is approximately 60% [43]. The energy model for this component of the EAF is relatively straightforward, as it involves the combustion of either natural gas or hydrogen.

The oxy-gas burner model is parameterized by the amount of natural gas used, establishing the corresponding mass and energy balances. For the mass balance, the chemical equation for the combustion of natural gas is considered, expressed as follows:

$$CH_4 + 2O_2 \rightarrow CO_2 + 2H_2O \tag{23}$$

For the energy contribution the corresponding lower heating value of the fuel has been used.

$$Q_{oxy-gasburner} = m_{NG} \times LHV_{NG} \tag{24}$$

As discussed in the literature review, the potential for using hydrogen as a heat source in the EAF to reduce carbon emissions is also examined. In this instance, the aforementioned formulas would be replaced with the following:

$$H_2 + \frac{1}{2}O_2 \rightarrow H_2O \tag{25}$$

$$Q_{oxy-gasburner} = m_{H_2} \times LHV_{H_2} \tag{26}$$

This model allows for the calculation of the energy contribution from both natural gas and hydrogen, with their respective shares determined by the parameter x_H_2. If x_H_2 is zero, the oxy-gas burner relies entirely on natural gas for its energy. Conversely, if x_H_2 is one, hydrogen combustion provides all the energy.

Intermediate values of x_H_2 represent a mix of both energy sources.

3.1.3 Oxygen Lancing

The introduction of oxygen into the melt initiates the oxidation of impurities, resulting in the formation of slag. The presence of lime and dolomite further contributes to the slag composition. Additionally, the exothermic nature of these oxidation reactions adds to the energy mix in the EAF. In this model, lime and dolomite are fully absorbed by the slag, ensuring no residual material remains in the melt.

Two primary inputs are considered: the oxygen introduced into the furnace and the composition of the melt. Parameter x_O_2 is used in the model to facilitate a sensitivity analysis regarding the quantity of oxygen introduced. This parameter represents the variation in oxygen injection from the initial values.

Oxygen lancing is responsible for numerous chemical reactions within the EAF. To simplify the model, the mass of each component undergoing oxidation to form slag is calculated by subtracting the total input of that element from the total amount present in the final composition of steel, as shown in equation 27. This calculation allows for the determination of the total amount of components that will oxidize to generate slag. The various components and oxidation reactions, along with the exothermic energy released by these processes, are detailed in Section 2.2.1. This applies to components such as Si, P, Cr, Mn, Al, Mo, and S. For iron oxide, the degree of oxidation depends on the quantity of oxygen injected into the furnace. A parameter has been developed to quantify the amount of oxygen consumed by the oxidation of iron. According to the literature, this parameter is typically around 0.32, indicating that 32% of the total oxygen fed into the furnace reacts to form iron oxide [44].

$$m_{i_{slag}} = m_{i_{iinput}} - m_{i_{steel}} \tag{27}$$

$$m_{O_{2_{FeO}}} = 0.32 m_{O_2} \tag{28}$$

Moreover, the total energy absorbed by the system as a result of oxygen lancing is determined by the following equation:

$$\begin{aligned} Q_{oxygen\ lancing} &= m_{Si_{slag}}\Delta H_{SiO_2} + m_{P_{slag}}\Delta H_{P_2O_5} \\ &+ m_{Cr_{slag}}\Delta H_{Cr_2O_3} + m_{Mn_{slag}}\Delta H_{MnO} \\ &+ m_{Al_{slag}}\Delta H_{Al_2O_3} + m_{Mo_{slag}}\Delta H_{MoO_2} \\ &+ m_{S_{slag}}\Delta H_{SO_2} + m_{Fe_{slag}}\Delta H_{FeO} \end{aligned} \tag{29}$$

Equation 29 represents the total energy input of oxygen lancing in the system. To calculate its contribution to the melt, this energy contribution is multiplied by the literature-based value of $\eta_{lo} = 0.8$ for the energy transfer efficiency factor [43].

3.1.4 Electrode Decomposition

During the operation of an Electric Arc Furnace, electrodes are used to transform electrical energy into thermal energy. The electrodes, composed of graphite, decompose directly in the melt, contributing to the thermal energy input as they oxidize to carbon dioxide (CO_2). The complete oxidation of the carbon from the electrodes results in the transfer of all the energy released by this exothermic reaction to the melt. As a result, the carbon dioxide produced contributes to the emissions from the furnace.

The decomposition of electrodes is correlated with the furnace's electricity consumption. It has been demonstrated that the generation of one tonne of steel at a power consumption of 390 kWh results in the decomposition of 3 kg of the electrode [8]. A linear regression model has therefore been developed to calculate the rate of electrode decomposition based on the electrical consumption of the furnace. It is recognized that several factors contribute to electrode decomposition, with electricity consumption representing a significant influence. For analysis, the function has been simplified as set out. Once the mass of electrode decomposition is determined, its energy contribution to the system can also be calculated.

$$Q_{electrode\ decomposition} = m_{C_{electrode}} \Delta H_{CO_2} \tag{30}$$

3.1.5 Carbon Injection

Carbon injection serves two primary purposes in the EAF. Firstly, it reduces the amount of iron oxide in the melt produced by oxygen lancing, thereby increasing the yield of steel. Secondly, the injected carbon oxidizes in the melt with oxygen, creating carbon monoxide (CO) bubbles. These bubbles generate a foamy slag that enhances heat transfer. Additionally, this process releases energy to both the melt and the off-gas from the system.

In this context, the carbon introduced by the metal (scrap and DRI) is also evaluated in conjunction with the injected carbon. The two types of injected carbon influence the various energy transfer efficiencies of the system. In addition, the presence of carbon in the different metals is not distributed in the same way, as discussed in Section 2.2.2.

In this context, the carbon introduced by the feedstock materials (scrap and DRI) is also evaluated alongside the injected carbon. Both types of carbon input—carbon injected directly into the furnace and carbon present in the feedstock materials (scrap and DRI)—affect the energy transfer efficiencies within the system. The distribution of carbon varies among different materials, as detailed in Section 2.2.2. This variation influences the overall energy dynamics, including the reduction of iron oxide and the formation of foamy slag.

Regarding the carbon contribution from scrap, the amount of carbon dissolved in the melt is determined as follows:

$$m_{C_{dissolve}} = m_{C_{input}} - m_{C_{steel}} \tag{31}$$

Once the amount of dissolved carbon is determined, it is oxidized to carbon monoxide (CO), contributing to the energy transfer as follows:

$$Q_{C_{scrap}} = m_{C_{dissolve}} \Delta H_{CO} \tag{32}$$

The carbon content of DRI comprises 20% free carbon. However, due to the continuous charging of DRI into the furnace, this free carbon is combusted directly in the freeboard as carbon dioxide (CO_2), and thus does not contribute to the steel composition. Conversely, cementite (Fe_3C) dissociates in the melt and subsequently reacts with other elements through chemical reactions.

$$Q_{C_{DRI_{Fe_3C}}} = 0.8 m_{C_{DRI}} \Delta H_{dissociation} \tag{33}$$

$$Q_{C_{DRI_{Free_C}}} = 0.2 m_{C_{DRI}} \Delta H_{CO} \tag{34}$$

The dissociated carbon from cementite subsequently reacts with iron oxide in the slag, contributing to a reduction in slag mass. In addition to the carbon introduced into the furnace via the metal charge, carbon is also injected directly into the furnace. The parameter k_C_CO has been developed to quantify the extent to which the injected carbon and carbon from the melt react to reduce iron oxide and how much contributes to the formation of CO bubbles in the presence of oxygen.

$$FeO + C \rightarrow Fe + CO \tag{35}$$

$$Q_{C_{FeO}} = (0.8 m_{C_{DRI}} + m_{C_{inj}}) * (1 - K_{C-CO}) \Delta H_{CO} \tag{36}$$

$$C + \frac{1}{2} O_2 \rightarrow CO \tag{37}$$

$$Q_{C_{inj_{CO}}} = m_{C_{inj}} K_{C-CO} \Delta H_{CO} \tag{38}$$

Both reactions result in the formation of CO bubbles, with the distinction that equation 39 represents an endothermic reaction, thereby absorbing energy from the system.

During the carbon injection process, various carbon sources are introduced. The resulting carbon monoxide undergoes a chemical reaction to form carbon dioxide, contingent upon the availability of oxygen in the furnace.

$$CO + \frac{1}{2}O_2 \rightarrow CO_2 \tag{39}$$

$$Q_{CO_{CO_2}} = m_{CO}\Delta H_{CO_2} \tag{40}$$

Thus, all reactions of carbon injection are developed and the total energy balance is as follows:

$$Q_{C_{inj}} = Q_{C_{scrap}} + Q_{C_{DRI_{Fe_3C}}} + Q_{C_{DRI_{Free_C}}} + Q_{C_{inj_{FeO}}} + Q_{C_{inj_{CO}}} + Q_{CO_{CO_2}} \tag{41}$$

While the energy balance presented applies to the entire furnace, it is not possible to simplify the energy contribution to the melt into a single efficiency parameter that accounts for the totality of the chemical reactions occurring in the furnace. To calculate the energy transferred to the melt from carbon injection, the following energy balance is established.

$$\begin{aligned} Q_{C_{\text{inj-melt}}} = \eta_{melt}(Q_{C_{\text{scrap}}} + Q_{C_{\text{DRI}_{Fe_3C}}} + Q_{C_{FeO}}) \\ + \eta_{CO}Q_{C_{\text{inj}_{CO}}} + \eta_{PC}(Q_{C_{\text{DRI}_{\text{Free}_C}}} + Q_{C_{CO_{CO_2}}}) \end{aligned} \tag{42}$$

3.1.6 Losses in the system

Energy is lost from the electric arc furnace through the walls and roof of the furnace and through the cooling system. As evidenced in the literature, the calculation of such losses is a challenging task, particularly given the difficulty in making precise predictions. Consequently, a ratio has been established whereby the losses of the system account for 10% of the total energy input to the furnace.

$$Q_{losses} = 0.1 Q_{total} \tag{43}$$

3.2 Reheating Furnace

The reheating furnace, as introduced in section 2.2.4, aims to reheat the slabs from the steel-making process to the hot rolling temperature of 1250 °C. This is usually done by burning natural gas, which will be the state-of-the-art technology to be examined and will be compared with a reheating furnace using hydrogen combustion and also plasma torch as potential decarbonization technologies.

3.2.1 Reheating Furnace with Recuperator

Essentially, the reheating furnace remains the same regardless of the fuel used. The primary focus of the study is to identify the most energy-efficient and least carbon-intensive fuel, as the specifications of the furnace itself remain constant. Figure 3.5 shows the structure of the energy model used. Two system boundaries can be identified. System Boundary 1 includes both the reheat furnace and the recuperator, while System Boundary 2 includes only the reheating furnace.

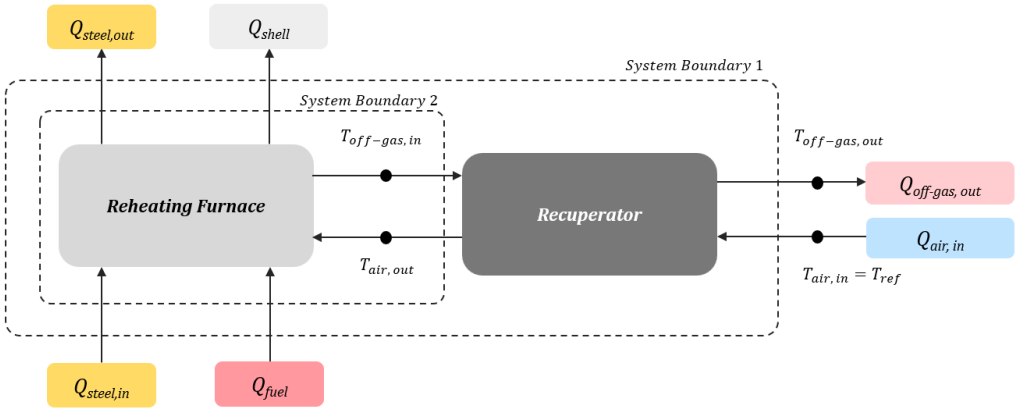

Figure 3.5: Energy Model and System Boundaries for the Reheating Furnace with a Recuperator

The energy balance of the model for system boundary 1 is described as follows:

$$Q_{total} = Q_{in} = Q_{out} \tag{44}$$

$$Q_{in} = Q_{steel_{in}} + Q_{fuel} \tag{45}$$

$$Q_{out} = Q_{steel_{out}} + Q_{shell} + Q_{off-gas} \tag{46}$$

Steel enters the furnace at temperatures between room temperature and 800°C. Therefore, the total energy absorbed by the steel entering the furnace ($Q_{steel,in}$) is denoted as

$$Q_{steel,in} = m_{steel} \times \int_{T_{ref}}^{T_{steel_{in}}} c_{p_{steel}}(T)\, dT \tag{47}$$

On the other hand, the shell losses of the system (Q_{shell}) also depend on the temperature of the steel entering the furnace. A simple linear regression analysis was performed to establish the relationship between the temperatures of the steel entering the furnace and the resulting system losses.

The inlet temperature and mass of the air entering the recuperator are known. The reference temperature is set to 20 °C, while the temperature of the off-gas leaving the furnace ($T_{off-gas,in}$) is set to 900 °C. With these values, the temperature of the preheated air in the furnace can be calculated using the Formula 48 with $\varepsilon = 0.5$. In this case, the calculated temperature is 460°C.

$$\varepsilon = \frac{T_{air_{out}} - T_{ref}}{T_{off-gas_{in}} - T_{ref}} \tag{48}$$

From here, the model works with System boundary 2 where the energy balance is:

$$Q_{total} = Q_{in} = Q_{out} \tag{49}$$

$$Q_{in} = Q_{steel_{in}} + Q_{fuel} + Q_{air_{out}} \tag{50}$$

$$Q_{out} = Q_{steel_{out}} + Q_{shell} + Q_{off-gas_{in}} \tag{51}$$

This allows different values of energy provided by the fuel to be tested. Once the energy required is known, the amount of natural gas can be calculated and with this, the rest of the mass balance can be determined. This allows the recalculation of the energy balance for the composition of the off-gas. When the minimum error is found, the code breaks and the amount of fuel required is determined. This loop is shown in Figure **??** for natural gas and hydrogen combustion.

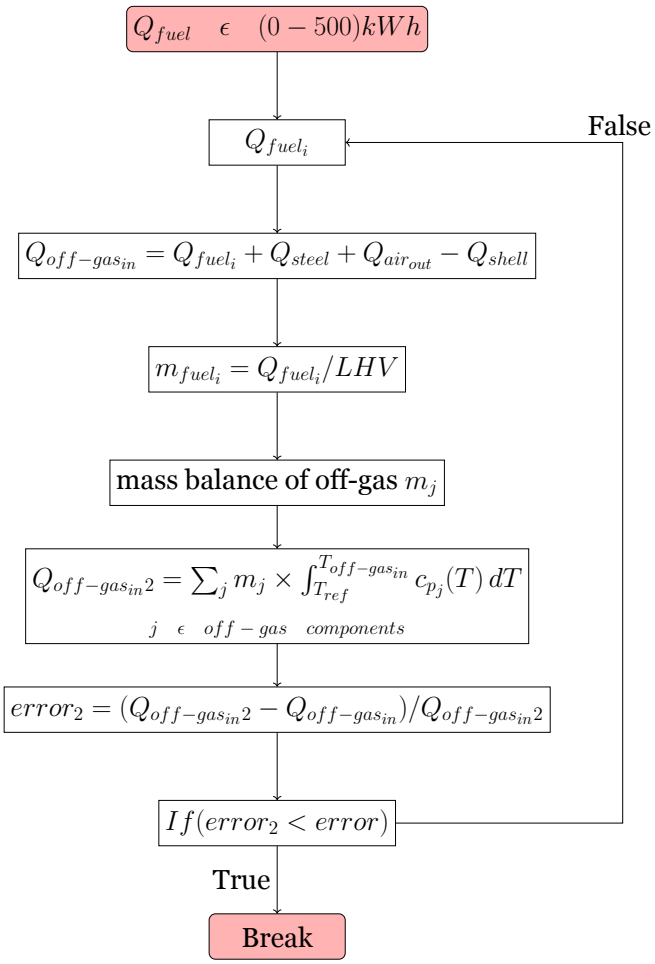

Figure 3.6: Loop in reheating furnace model for hydrogen and natural gas combustion

To calculate the reheating furnace energy and mass balance for plasma heating, a similar loop was constructed. The primary discrepancy is observed in the calculation of the mass of nitrogen required to power the system. In this case, nitrogen is not combusted. Instead of using the lower heating value to determine the amount of fuel required, the mass of nitrogen is calculated by considering the heat required and deriving the mass of nitrogen required from the specific enthalpy of nitrogen at the plasma temperature, which is typically 11.6 thousand Kelvin. On the other hand, once the amount of energy required has been determined, the electrical consumption of the plasma torch can be calculated as follows:

$$Q_{el_{plasma}} = Q_{fuel}/\eta_{plasma\ torch} \tag{52}$$

Being the efficiency of the plasma torch of 90%. In Figure 3.7 the corresponding loop for the plasma heating calculation is shown.

As for the calculation of the enthalpy of nitrogen at a given temperature, the data based on Figure 3.8 has been used.

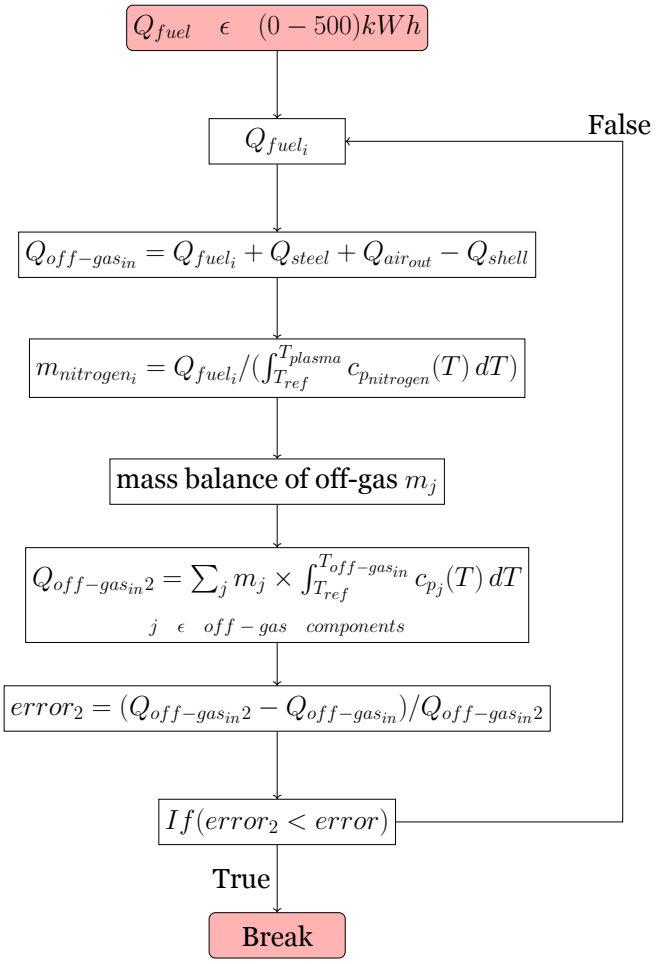

Figure 3.7: Loop in reheating furnace model for nitrogen plasma

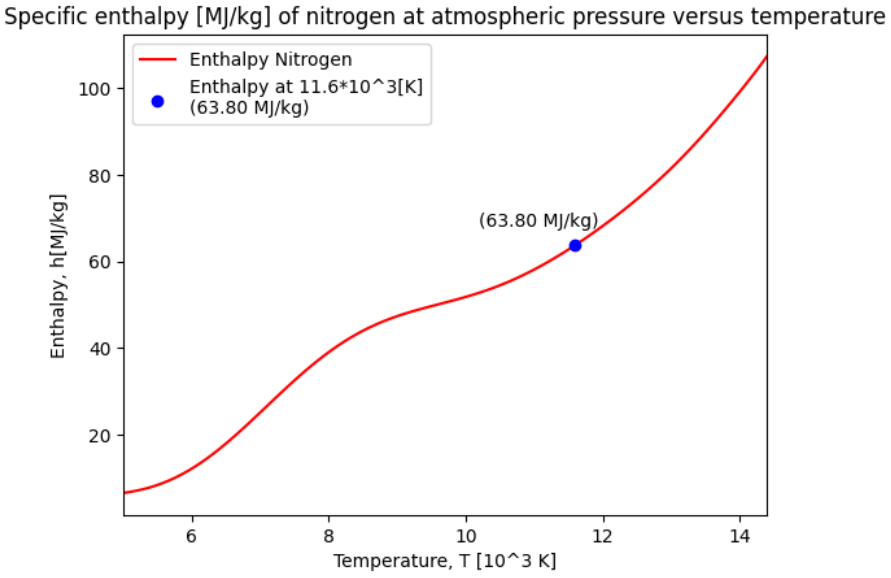

Figure 3.8: Nitrogen Plasma Specific Enthalpy [45]

3.2.2 Reheating Furnace with Off-gas from EAF

A second energy model has been developed using the EAF off-gas to assist in heating the steel slabs in the reheating furnace when considering the energy integration of the mini-mill. In this case, the recuperator has been ignored since the gas entering the furnace will in most cases be at a higher temperature than the exhaust from the system. This eliminates the possibility of preheating the gas entering the furnace. Figure **??** shows the energy model along with the system boundaries.

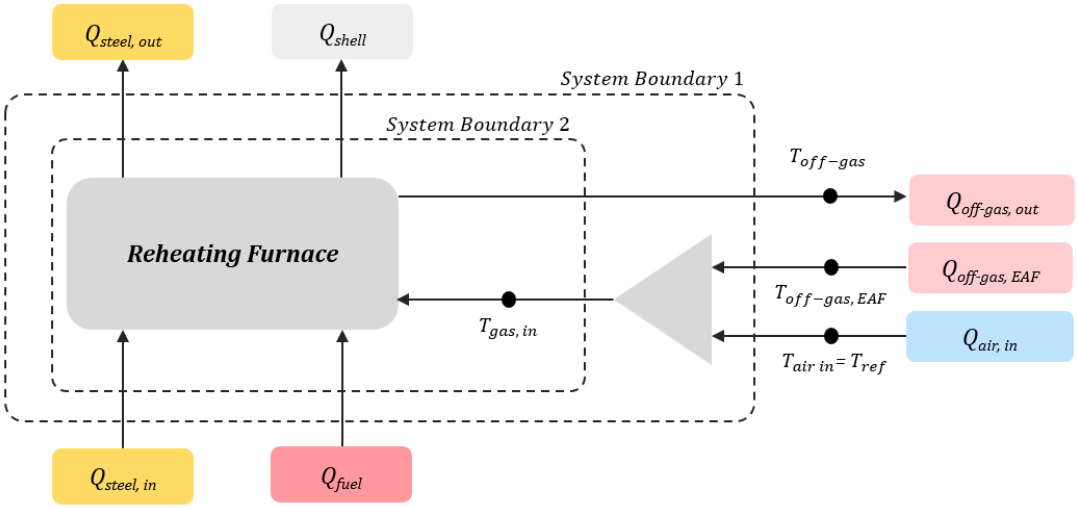

Figure 3.9: Energy Model Reheating Furnace with Off-gas

In this model, the energy model first solves for the air-gas mixer, which results in the combined enthalpy of the two streams. Once the mass and energy balance of the air-gas mixer is solved, the result is used as an input to the reheating furnace model. The same loops as in section 3.2.1 are used in this model, although the energy balance differs from the previous model in which pure air entered the furnace. In this case, the calculated gas enthalpy is used. The rest of the process remains the same. Once again, the three types of fuel were tested.

$$Q_{gas_{in}} = Q_{off-gas_{out}} + Q_{air_{in}} \tag{53}$$

First of all the mass balance will be resolved as:

$$m_{gas_{in}} = m_{off-gas_{out}} + m_{air_{in}} \tag{54}$$

One the mass balance of the air-gas mixer is known, the heat balance of the mixer is calculated as follows.

$$Q_{gas_{in}} = \sum_i m_i \times \int_{T_{ref}}^{T_{off-gas_{out}}} c_{p_i}(T)\, dT;\ i \quad \epsilon \quad off-gas \quad components \tag{55}$$

With the mass and energy balance solved, the heat required from the fuel is calculated in the same way as in the previous system, using the formulas from the reheating fuel loop.

3.3 Preheating Furnace

The objective of the preheating furnace is to elevate the temperature of the feed metal in the EAF to the point where the EAF utilizes energy primarily for melting and not for heating the feed. As the preheating furnace operates on the same fundamental principles as a reheating furnace, the energy model is identical. Its impact on the Electric Arc Furnace is evaluated based on the temperature of the metal entering the furnace. Therefore:

$$Q_{steel_{in_{EAF}}} = Q_{steel_{out_{PH}}} \tag{56}$$

$$m_{steel_{in_{EAF}}} \times \int_{T_{ref}}^{T_{steel_{in_{EAF}}}} c_{p_{steel}}(T)\, dT = m_{steel_{out_{PH}}} \times \int_{T_{ref}}^{T_{steel_{out_{PH}}}} c_{p_{steel}}(T)\, dT \tag{57}$$

Two constraints must be taken into account when evaluating the system: the preheating furnace and the Electric Arc Furnace. The two constraints to be considered are as follows: firstly, the temperature of the steel exiting the preheating furnace must be equal to that of the steel entering the EAF; secondly, the mass of steel must be the same for both processes.

Consequently, the electrical consumption of the EAF will be significantly reduced, necessitating an assessment of the overall system energy requirement to evaluate the potential of the preheating furnace as a decarbonization strategy.

4 Results

This chapter presents a discussion of the results obtained from the application of the various models. First, the energy consumption of the models is presented and validated with literature. Subsequently, the potential for decarbonization and economic competitiveness are evaluated.

The energy consumption results will be accompanied by the decarbonization potential as they are closely related. The decarbonization potential is evaluated by taking into account the carbon dioxide emissions of the system (e.g. combustion of carbon in the furnace, combustion of natural gas) in addition to the carbon dioxide emissions from the electricity grid to compare the different cases. The carbon dioxide emissions associated with renewable electricity consumption are not included, as they are known to be zero.

The impact of electricity emissions is considered in relation to two countries. The present study focuses on Germany and Sweden as case studies. In the context of the European Union, these two countries represent the most significant efforts towards the production of green steel. Furthermore, the two countries differ significantly regarding their respective electricity grids. Germany presents a high carbon intensity grid with 349.78 gCO_2/kWh el, due to a high percentage of electricity produced by coal and natural gas [46]. Conversely, the Swedish grid, with 40.7 gCO_2/kWh el, is one of the least carbon-intensive grids globally, largely due to electricity generation from predominantly low-carbon sources [46]. The objective of examining these different cases is to demonstrate the impact of different electricity generation sources on the potential for decarbonization through electrification.

4.1 EAF

To evaluate the energetic and decarbonization potential of the EAF model, it is essential to determine the parameters kC_CO, kO2_FeO, and kO2air_CO2. A systematic looping process was employed to analyze the impact of these parameters on the model, facilitating precise parameter tuning.

To establish the parameter tuning loop, the results from the model were compared

Parameter	Description
kC_CO	Proportion of carbon that is combusted to carbon monoxide
kO2_FeO	Proportion of lanced oxygen that is oxidizing iron
kO2air_CO2	Proportion of oxygen from infiltrated air that is combusted to carbon dioxide

Table 4.1: Parameter description

Mass Slag [kg]	78
Mass Off-gas [kg]	235
Mass Liquid Steel [kg]	1000
Chemical Energy [kWh]	314
Electrical Energy [kWh]	393
Energy Off-gas [kWh]	168
Energy Slag [kWh]	31
Energy Liquid Steel [kWh]	397

Table 4.2: Optimal System Results

with those from the literature and an error of the system was calculated. The results evaluated are those shown in the table 4.2.

To evaluate the error of the model, the weighted sum of the relative errors between the model's predicted values and the corresponding literature values are calculated. The formula used for the error calculation is defined as follows:

$$\text{Error} = \sum_{i=1}^{n} w_i \cdot \left| \frac{M_i - L_i}{L_i} \right|$$

Where:

- M_i represents the model's predicted value for the ith term.
- L_i represents the literature value for the ith term.
- w_i is the weight assigned to the ith term. If no specific weights are provided, equal weights ($w_i = 1$ for all i) are used.
- n is the total number of terms being compared.

This formula calculates the absolute relative error for each term, multiplies it by the corresponding weight, and then sums these weighted errors to obtain the total error for the model.

A parameter tuning loop has been conducted to assess the optimal parameterization of kC_CO & kO2_FeO. The values have been validated across all combinations from 0 to 1, as illustrated in Figure 4.1.

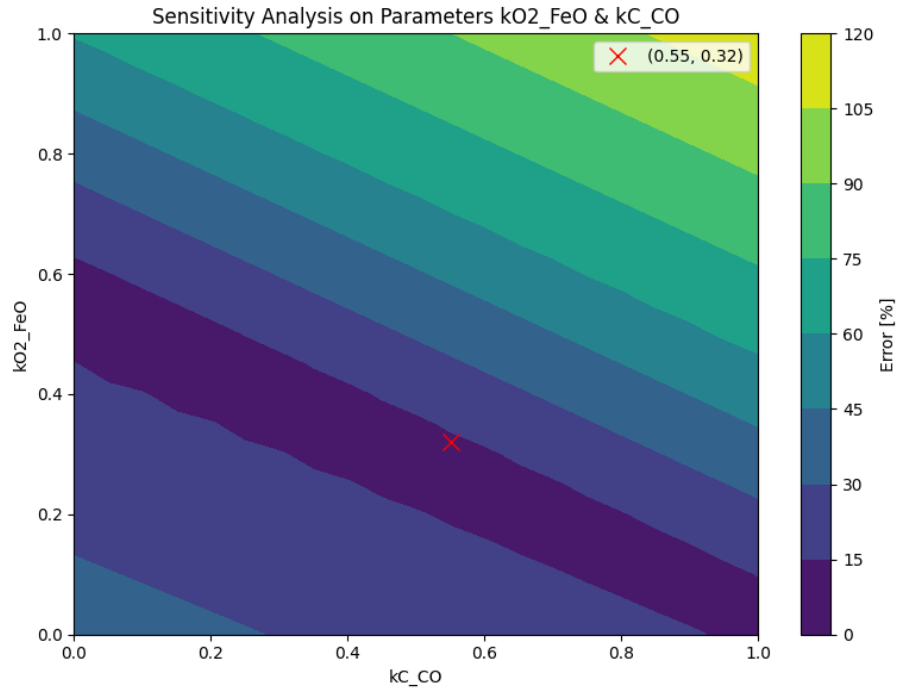

Figure 4.1: Sensitivity Analysis for parameters kC_CO & kO2_FeO

As shown in Figure 4.1, the range of cumulative error is between 0 and 120%, which underscores the importance of proper parameterization in the system. In addition, Figure 4.1 shows a strong correlation between the parameters kC_CO and kO2_FeO. Consequently, the optimal solution is defined by using the literature value kO2_FeO = 0.32 and parameterizing kC_CO by the combination with the least error. This led to the final parameterization of kC_CO = 0.55.

The parameterization of kO2air_CO2 is considered separately from the previous two. It is mainly used in the evaluation of the off-gas of the system. A sensitivity analysis of the kO2air_CO2 parameter has been performed, and the literature indicates that the ratio between carbon monoxide and carbon dioxide in the off-gas is approximately 50 percent each. As can be seen in Figure 4.2, the optimal parameter for this is to keep kO2air_CO2 = 0 for scrap melting.

When evaluating DRI as an input the parametrization of this parameter changes slightly making its optimal value at kO2air_CO2 = 0.24

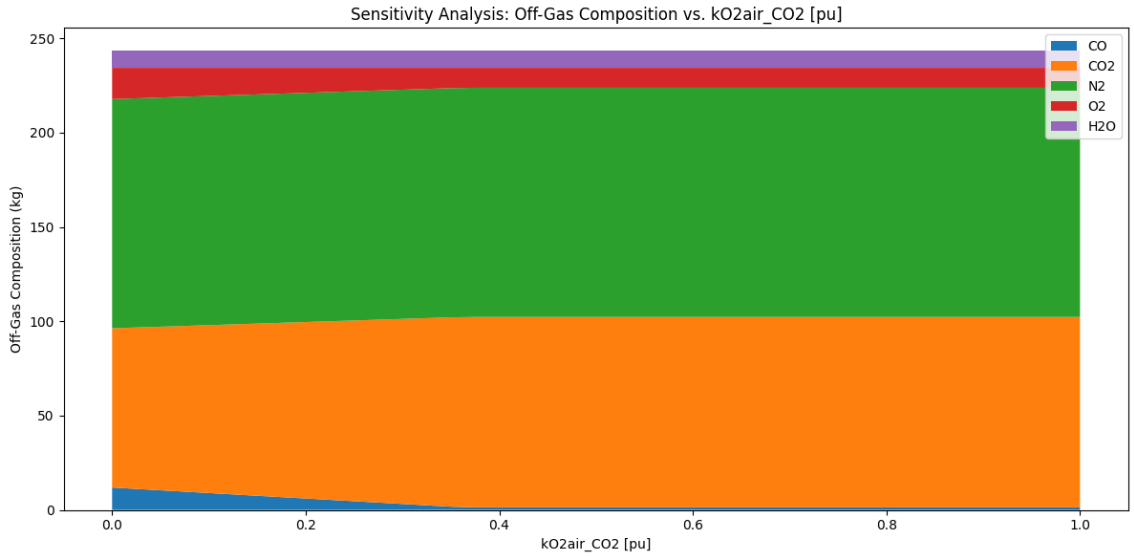

Figure 4.2: Sensitivity Analysis parameter kO2air_CO2

Now that the parameter tuning is complete, the next step is to examine the model's results.

First, the energy consumption results of the Electric Arc Furnace are evaluated when being fed by scrap as most of the literature energy models correspond to this case. Literature findings show that electrical energy consumption represents 65% of the total energy demand while the modeling results in this work generate 57% [47]. In Table 4.3, the results of the energy model and mass model are compared with literature results. It can be seen that although the electrical energy consumption has a wide range, the results from the model are well within the range obtained by literature.

In Table 4.3, it can be observed that the model aligns well with literature values overall. However, notable deviations are present in the Energy Slag results. This discrepancy may be attributed to the limited available data on the enthalpy of slag, indicating that this aspect of the model requires careful consideration. Another deviation from literature values is evident in the analysis of energy losses. The model shows significantly lower energy losses, which could be due to the inherent difficulty in accurately calculating losses in the EAF system as reported in the literature [43]. Therefore, substantial deviations are to be expected.

Table 4.4 presents the final composition of slag, compared with values reported

	Literature	Model	References
Electrical Energy [kWh/t steel]	393, 375, 450, 300-550, 467	393.48	[8], [29], [47], [48], [49]
Chemical Reactions [kWh/t steel]	314, 201	215.78	[8], [49]
Electrodes [kWh/t steel]	28, 16	27.10	[8], [49]
Natural Gas Burners [kWh/t steel]	50, 70	52.40	[8], [49]
Energy Liquid Steel [kWh/t steel]	397, 391	406.56	[8], [49]
Energy Slag [kWh/t steel]	31, 42	90.97	[8], [49]
Energy Off-gas [kWh/t steel]	168, 121	145.32	[8], [49]
Energy Losses [kWh/t steel]	177, 207, 132	106.99	[8], [49], [50]
Liquid Steel [kg]	1000	976.89	[8]
Off-gasses [kg]	235	229.22	[8]
Slag [kg]	78	85.40	[8]
Temperature Off-gas [K]	2000	2190.00	[51]

Table 4.3: Results EAF for scrap as the input metal

in the literature. It is evident that the literature accommodates a broad range of parameters as standard. This variability is attributed to several factors, including the type of steel entering the furnace and the quantities of dolomite, lime, carbon, and oxygen used. It can be seen that the model results are well within the margins set by literature.

	Literature	Model	References
CaO [%]	2.3-60, 15-50	28.98	[52, 53]
Al_2O_3 [%]	2-22.6, 2-15	5.76	[52, 53]
MgO [%]	3-15, 1-13	6.97	[52, 53]
SiO_2 [%]	5-32, 4-25	9.59	[52, 53]
FeO [%]	1-50.9, 15-42	48.00	[52, 53]
MnO [%]	0.4-15.6, 0.5-19.5	0.64	[52, 53]

Table 4.4: Composition Slag

Figure 4.3 shows a summary of the results from the EAF model input of different metals. It can be seen that the power consumption increases significantly when DRI metal is fed into the furnace compared to scrap feeding. This is due to the higher heat required to melt DRI compared to scrap. As discussed in Section 3.1, the energy transfer efficiency of in-situ carbon of DRI is higher than that of the injected carbon. This represents an advantage over carbon injection, although it

is not visible in the results due to the high energy required to melt DRI. Referring to the results of H2-DRI, it can be seen that the power consumption is higher compared to DRI due to lack of carbon in its composition. A more in-depth study on H2-DRI is required as it is known that it requires more energy to melt compared to natural gas-based DRI. In addition, slag is not as foamy due to the lack of carbon, which results in poorer transfer efficiency from the arcs to the melt, requiring additional energy. Therefore, the results of H2-DRI are preliminary and need to be complemented.

A notable decrease in steel yield can be observed when comparing the results of DRI and H2-DRI with those of scrap. This is primarily attributable to the fact that DRI contains a greater proportion of gangue (invaluable material that surrounds or is mixed with the valuable mineral) in its structure than scrap, which consequently increases the slag produced by the system. A comparison of the steel yield of H2-DRI with that of DRI reveals that the lower carbon in situ in H2-DRI results in a reduced iron recovery from the slag. Consequently, the same steel yield as that achieved with DRI requires a greater quantity of carbon injection.

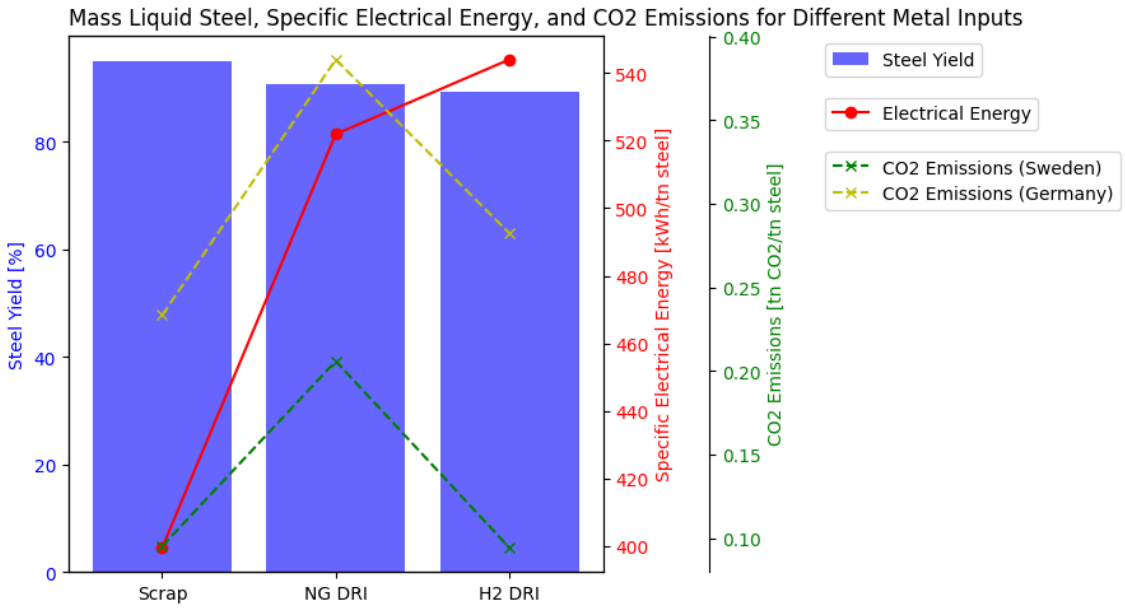

Figure 4.3: Results EAF with Different Input Metals

This study finally analyzes the emissions resulting from the three metal inputs. The primary distinction is based on the in situ carbon content of DRI, which markedly elevates the emissions of DRI in comparison to the other two metal

inputs. It is evident that H2-DRI generates greater emissions than scrap due to its higher electricity demand. However, if a scenario with 100% renewable electricity were to be considered, it would be observed that the emissions from melting H2-DRI would be lower than those of scrap, as the carbon in situ in scrap would not be present to oxidize and contribute to the system emissions. The ranges of emissions from an electric arc furnace (EAF) in the literature are approximately 0.1 to 0.2 tons of carbon dioxide t CO_2/t of steel when scrap is used as the input metal, as cited in reference [4].

Finally, the emissions of the three metal inputs are analyzed. The main difference is based on the in-situ carbon of DRI, which significantly increases the emissions of DRI compared to the other two metal inputs. It can be seen that H2-DRI produces more emissions than scrap due to the higher electricity requirement, although if a scenario with 100% renewable electricity would be taken into consideration it would be seen that the emissions from melting H2-DRI would be lower than that of crap as the carbon in situ in scrap would not be there to oxidate and contribute the system emissions. The ranges of EAF emissions in the literature are around 0.1-0.2 t CO_2/t of steel when scrap is used as the input metal [4]. From the results, it can be seen that the Swedish case corresponds to the lower limit while the German case corresponds to the upper limit.

4.2 Reheating Furnace

In the following section, the energy model results are discussed along with the decarbonization potential of the reheating furnace. As mentioned earlier, the reheating furnace is evaluated using three different fuels, natural gas, hydrogen, and plasma. The energy model for these three fuels is largely similar and the results are shown in table 4.5 and Figure 4.4. In table 4.5 the results for the three models are compared with literature values. Figure 4.4 shows the results of the natural gas reheating furnace in a more graphical way for the reader.

The results in table 4.5 show that the energy required from the fuel is slightly different in each case. The energy absorbed by steel is the same in all three cases because steel is heated to and from the same temperature. The energy of the preheated air is similar because the air is always preheated to the same

	Natural Gas [kWh]	Hydrogen [kWh]	Plasma [kWh]	Literature [kWh]
Fuel	423	427.35	401.70	396.94
Steel	249.45	249.45	249.45	229.71
Off-gas	169	173.35	147.70	170.69
Preheated air	67.68	67.68	67.68	67.48
Furnace Loss	72.77	72.77	72.77	63.11

Table 4.5: Energy balance Reheating furnace [6]

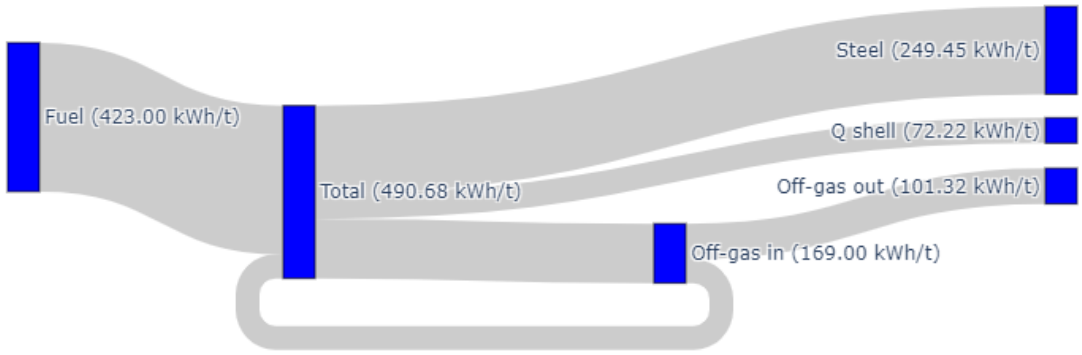

Figure 4.4: Graphic representation of energy model results in reheating furnace

temperature regardless of the fuel. The shell losses are the same for all fuels because the temperature inside the furnace is 1250 °C. The main difference is the composition of the off-gas. Different fuels produce different compositions of off-gases, so the energy lost to the environment and the energy required to power the system depends on the composition of the off-gas. Figure 4.5 shows the energy of the off-gas, taking into account their different enthalpies. The hydrogen combustion case has the highest energy content and therefore requires more fuel than the other cases. Plasma has a lower energy content because it contains only oxygen and nitrogen, which have significantly lower enthalpies than carbon dioxide or water vapor, which are present in the exhaust in the natural gas and hydrogen cases.

Figure 4.6 shows the result of the final energy demand for the three technologies. When the final energy demand from the hydrogen combustion in the furnace is considered, the final energy demand takes into account not only the energy required from the combustion of hydrogen but also the energy required to produce hydrogen and therefore the energy required to power the electrolyzer. On the

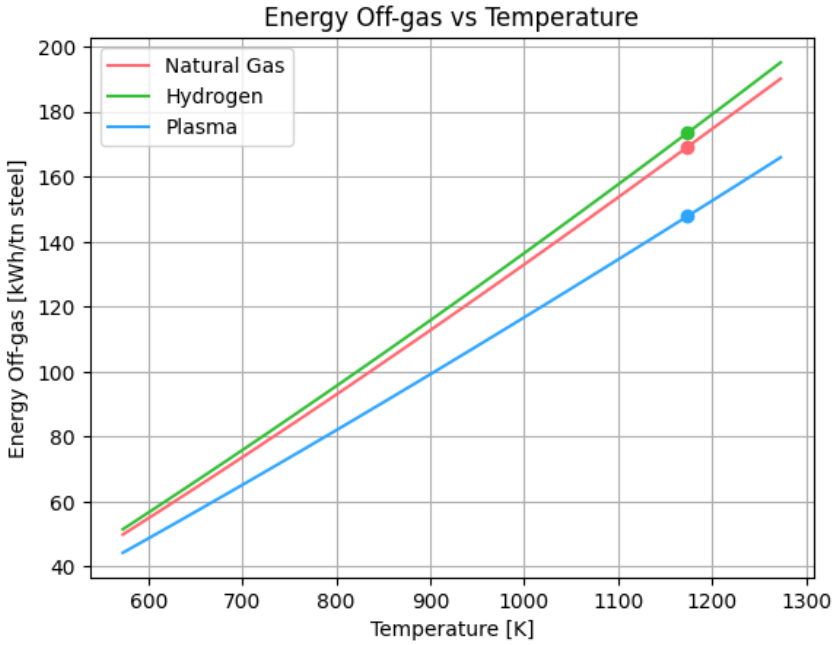

Figure 4.5: Energy in off-gas vs temperature

other hand, when the final energy demand from the plasma heating case is considered, similar to the hydrogen final energy demand, the calculation for plasma also takes into account the energy required to generate the plasma state and the energy required to produce nitrogen from air in a cryogenic air distillation unit. Figure 4.6 shows the energy intensities for the three cases and different metal slab inlet temperatures from 20 °C to 800 °C, considering direct casting to the reheating furnace.

Figure 4.6 illustrates that the production of hydrogen requires a considerable amount of energy, given the current state of technology. Consequently, this method is identified as the most energy-intensive approach for heating slabs in a reheating furnace. Conversely, it can be observed that while plasma requires less energy in the form of heat within the furnace (see Figure 4.5) compared to natural gas, the additional energy required to maintain the plasma state and produce nitrogen results in a greater overall energy demand than that of a natural gas reheating furnace.

From the decarbonization potential results, it can be seen that the decarbonization potential when utilizing electricity from the Swedish electricity grid is quite high, as in the hydrogen case there is a 67% reduction, and in the plasma case more than

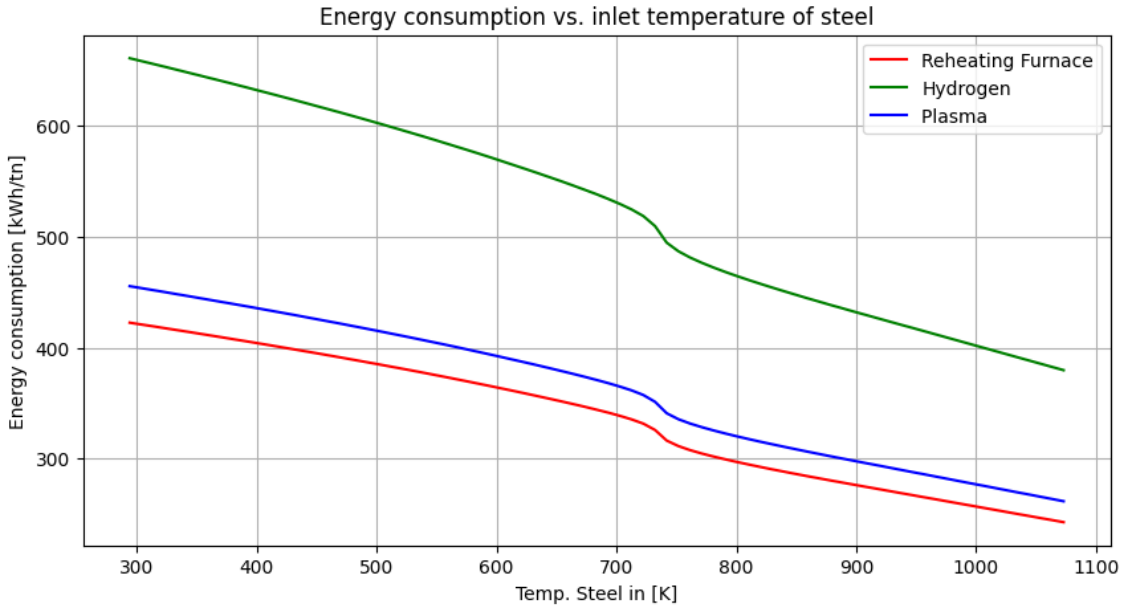

Figure 4.6: Energy consumption for different inlet temperature of steel slabs

75% emission reduction compared to the natural gas case. Looking at the total emissions when using the German electricity grid, as it is quite carbon-intensive, no decarbonization is achieved. This, however, will change in the future if they follow the planned grid decarbonization. Therefore, in countries like Germany, the implementation of renewable energy to power the steel mill is essential for the decarbonization of green steel production through electrification.

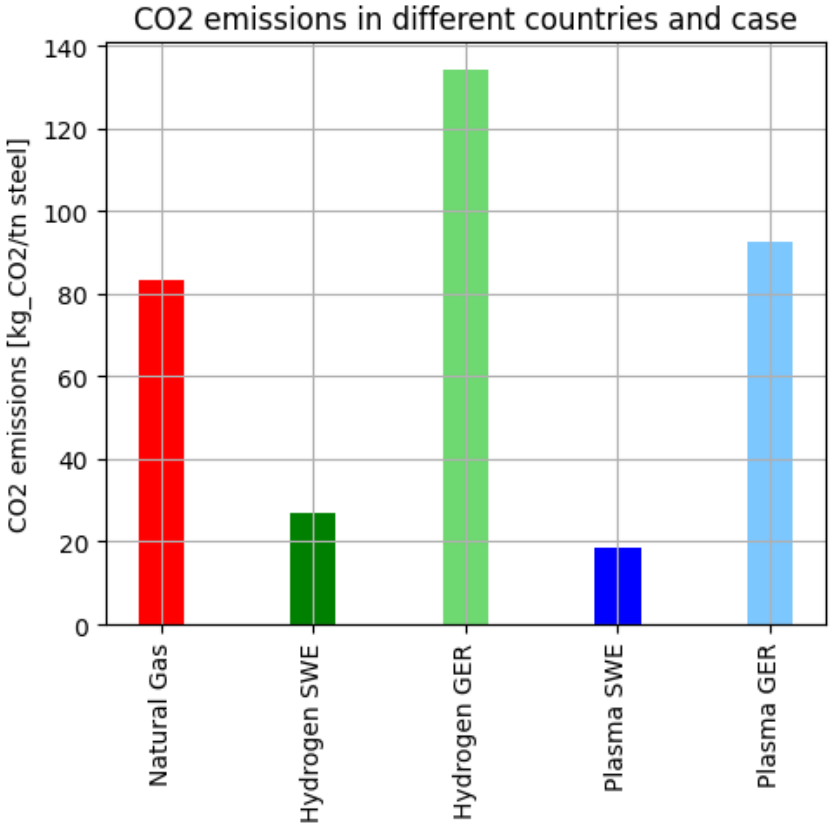

Figure 4.7: CO2 emissions for each case and with different electricity grids

4.3 Preheating EAF

To evaluate the energy consumption of the coupled system of the EAF with a preheating furnace and to determine the least energy-intensive solution, the energy consumption results of the preheating furnace are compared with the energy savings of the EAF due to the increased inlet temperature of steel. Figure 4.8 illustrates the energy required for preheating metal to 800 °C. The energy required for preheating is represented by the hatched bars, while the solid bars indicate the electrical energy required by the EAF to melt the metal. For comparison, the black dashed line represents the electrical energy consumed by the EAF when melting steel under typical operational conditions, without preheating.

Preheating scrap to 800 °C was chosen for evaluation, as higher preheating temperatures result in significant oxidation of the scrap and can cause CO explosions in the EAF [54]. It is notable that all configurations with preheating

furnaces are more energy-intensive than the option of inputting metal at room temperature. The EAF's electric energy requirement decreases by approximately 200 kWh per ton of steel. This finding is consistent with literature, which reports a reduction of 207 kWh per ton of steel when scrap is introduced at 800 °C [54].

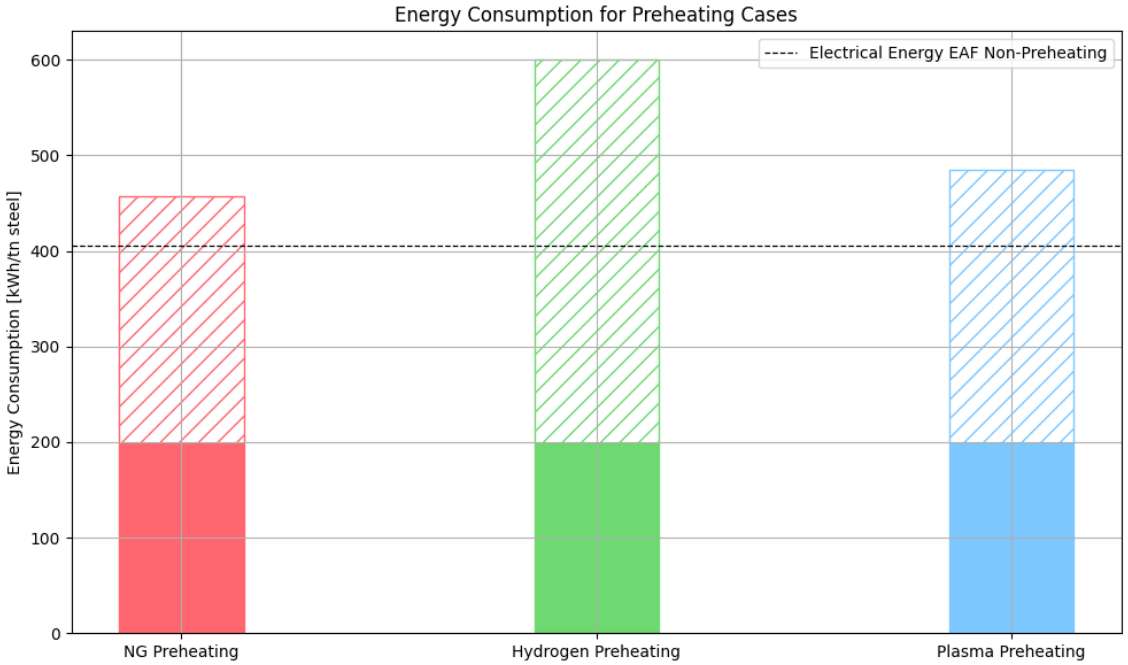

Figure 4.8: Energy Consumption for Preheating Cases

Figure 4.9 illustrates the discrepancy in emissions between the preheating and non-preheating scenarios within the contexts of the Swedish and German electrical energy grids. In Sweden, where the electricity grid has a minimal impact on emissions, the implementation of electrified preheating options does not significantly affect the system's emissions. This contrasts with the German case, where the more emission-intensive electricity grid results in a notable increase in indirect emissions due to the increment in electricity demand compared to the non-preheating scenario.

Regarding preheating via natural gas, it is noticeable that this option is less emission-intensive than the electrified alternatives in the German case, given that the electricity grid is relatively more emission-intensive even when compared to emissions from natural gas combustion. Conversely, in the Swedish case, the most emission-intensive scenario arises from natural gas preheating, as the country's

electricity grid is predominantly carbon-free. The advantages of metal preheating will be further elaborated upon in the economic analysis.

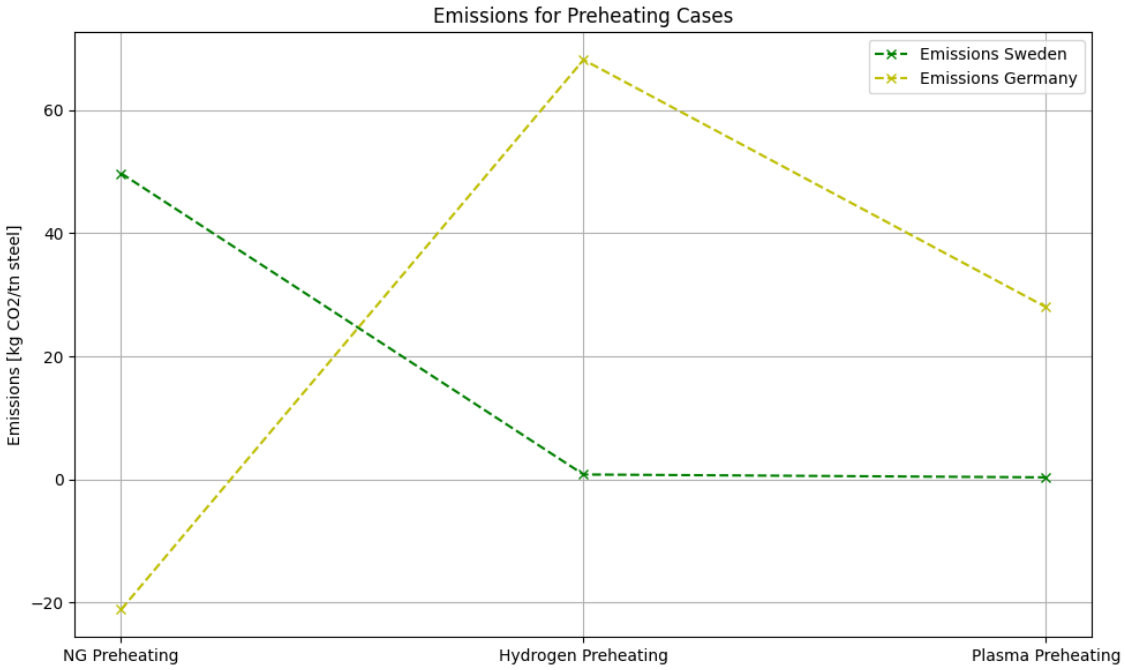

Figure 4.9: Decarbonization Potential for Preheating Cases

As observed in Figure 4.10 and Figure 4.11, the utilization of off-gas from the EAF in the preheating furnace results in further reductions in energy consumption and emissions. Figure 4.10 presents data on energy savings across all cases, while Figure 4.11 illustrates the decarbonization potential. The results indicate that preheating using the heat from the EAF off-gas has the potential to reduce the energy intensity of the preheating furnace and EAF compared to a non-preheating scheme. Additionally, this strategy demonstrates significant decarbonization potential.

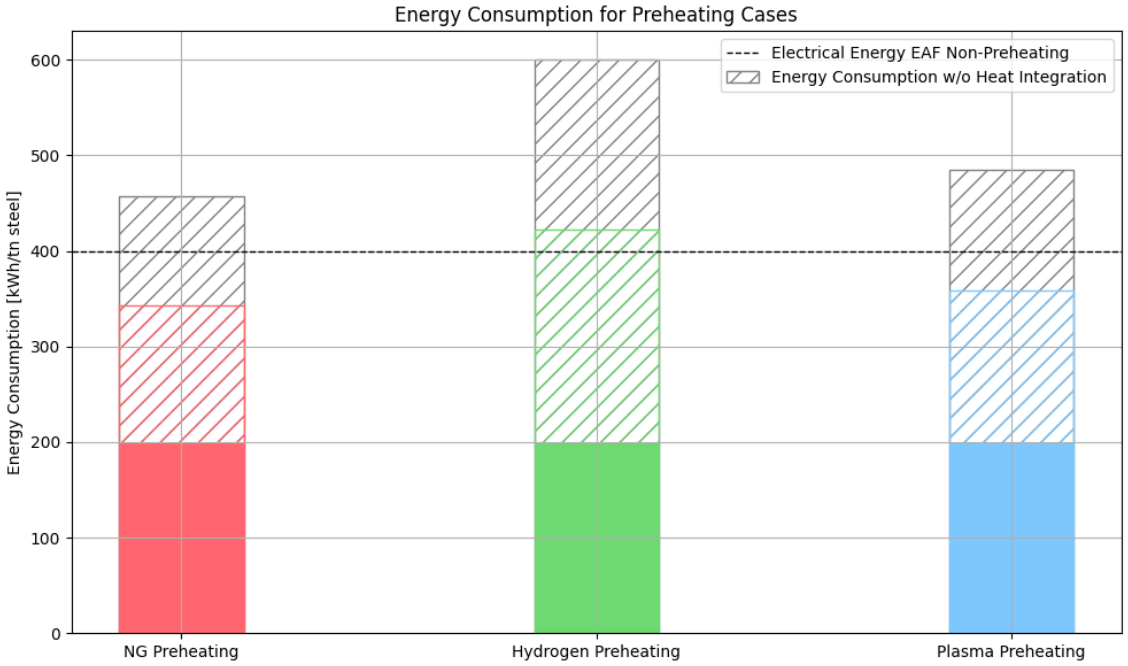

Figure 4.10: Energy Consumption for Preheating Cases Using Off-gas Heat

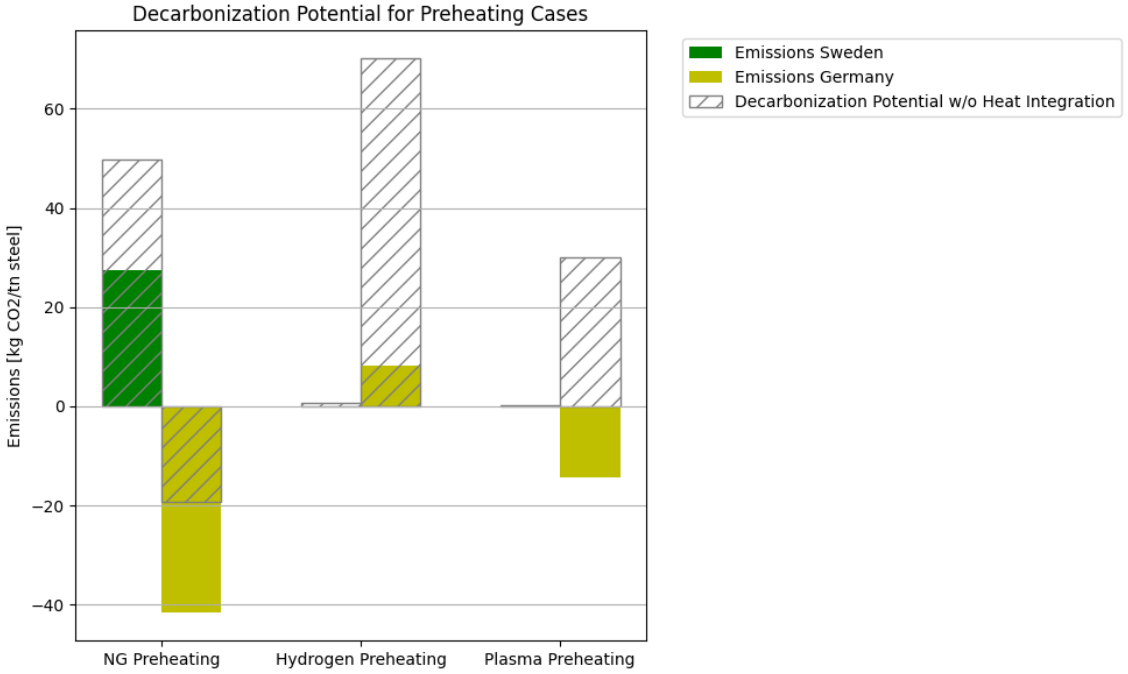

Figure 4.11: Decarbonization Potential for Preheating Cases Using Off-gas Heat

4.4 Economics

To evaluate the different electrification options for the overall mini-mill system, six configurations were developed. The first two scenarios are based on the current technologies employed in the mini-mill:

- Case-1 (NG): This configuration consists of a system with an EAF followed by a reheating furnace fired by natural gas.
- Case-2 (NG-Preheating): Similar to Case-1, this configuration also includes a preheating furnace fired by natural gas.

These two cases serve as baseline scenarios to contextualize the results of the electrification options. The subsequent scenarios explore the potential of hydrogen as an energy source:

- Case-3 (Hydrogen): This case evaluates the possibility of using hydrogen in the reheating furnace.
- Case-4 (Preheating Hydrogen): This configuration includes hydrogen combustion in both the preheating and reheating furnaces, as well as within the EAF, replacing natural gas.

The final scenarios investigate the use of plasma as an energy carrier:

- Case-5 (Plasma): This case utilizes plasma heating torches in the reheating furnace.
- Case-6 (Plasma Preheating): This configuration employs plasma heating torches in both the preheating and reheating furnaces.

These configurations provide a comprehensive framework to compare and understand the potential benefits and economic challenges associated with different electrification options for the mini-mill system.

The financial metric of Net Present Value (NPV) has been utilized to conduct the economic analysis. NPV evaluates the profitability of projects by calculating the present value of expected cash flows, considering the time value of money. This metric is essential for assessing the long-term economic viability of investments in new technologies. Since the project modifies only certain aspects of the

mini-mill system rather than the entire system, a differential approach was adopted. Consequently, the NPVs of the scenarios are presented relative to Case-1 (NG).

To calculate the NPV of a project, both Operational Expenditure (OpEx) and Capital Expenditure (CapEx) must be determined. OpEx includes costs such as fuel, electricity, and labor, while CapEx refers to investments made by a company to acquire, improve, or maintain physical and fixed assets. The following sections will detail these metrics in the context of the six developed cases.

4.4.1 OpEx

To calculate the OpEx for the developed scenarios, various industrial energy prices within the EU context were utilized. Electrifying a steel plant makes renewable energy a crucial asset for effectively reducing system emissions. Therefore, electrification can be approached in two ways:

- Grid Connected (GC): In this scenario, the steel plant is connected to an electricity grid. The operational costs are governed by the electricity prices of the region where the plant is located.
- Renewable Energy (RE): In this scenario, the steel plant installs various renewable technologies to power the plant. The costs are governed by the CapEx for installing renewables.

For this thesis, European prices have been used for the economic analysis. However, it is important to note that the conclusions from the economic study may vary depending on the specific region where the steel plant is located. For instance, the Levelized Cost of Hydrogen (LCOH) for a Grid Connected (GC) scenario in Sweden is currently lower than that for a Renewable Energy (RE) scenario. Therefore, for specific steel plants, this data may require further specification. Appendix A provides detailed information on country-specific European LCOH. Table 4.6 presents the costs of the various fuels utilized in the model.

When considering the EU ETS (carbon pricing), it is important to note that the steel industry is currently considered a carbon leakage risk industry, and therefore

Fuel	Cost	Reference
Coal	269.7 [EUR/t coal]	[55]
Natural Gas	32.3 [EUR/MWh]	[56]
Electricity (GC)	89.2 [EUR/MWh]	[57]
LCOE (RE)	70 [EUR/MWh]	[58]
LCOH (GC)	9.85 [EUR/kg H_2]	[59]
LCOH (RE)	7.09 [EUR/kg H_2]	[59]
Electrode	2763.03 [EUR/t electrode]	[60]

Table 4.6: Operational Expenditure (OpEx) 2024

carbon pricing does not currently apply to its production costs [61]. This is not expected to change in the near future, but carbon leakage from 2040 has been taken into account. The carbon price is currently set at 66.25 EUR/t CO_2 and it's expected to increase significantly in the future [62]. According to different estimates, by 2050, the carbon price is expected to be around 500 EUR/t CO_2 according to Enerdata [63], while Robert C. Pietzcker's estimates suggest that the carbon price should rise to 350 EUR/t CO_2 in order to achieve European Green Deal targets by 2050 [64].

When analyzing the operational costs of the mini-mill these have been extrapolated to a mini-mill plant of 200,000 t of steel produced per year. In Figure 4.12 the operational costs for the six scenarios over the next 25 years for GC scenario is shown.

Figure 4.12 depicts the potential impact of carbon pricing on the operating costs of mini-mills in the future. It suggests that natural gas-fired reheating furnaces may become uncompetitive with plasma reheating furnaces in the coming years. Furthermore, it can be observed that preheating schemas represent a cost-effective solution for all technologies. In the case of considering preheating furnaces using plasma heating technology, this is attributable to the fact that this system is less energy-intensive than the non-preheating system. In the case of natural gas-fired furnaces, however, the advantage of using a preheating furnace is not only due to the aforementioned factor but also to the fact that the energy provided by natural gas is cheaper than that of electricity. Finally, the results for the preheating case using hydrogen combustion demonstrate that this schema is cost-effective due to the electrode's reduced decomposition. This makes hydrogen

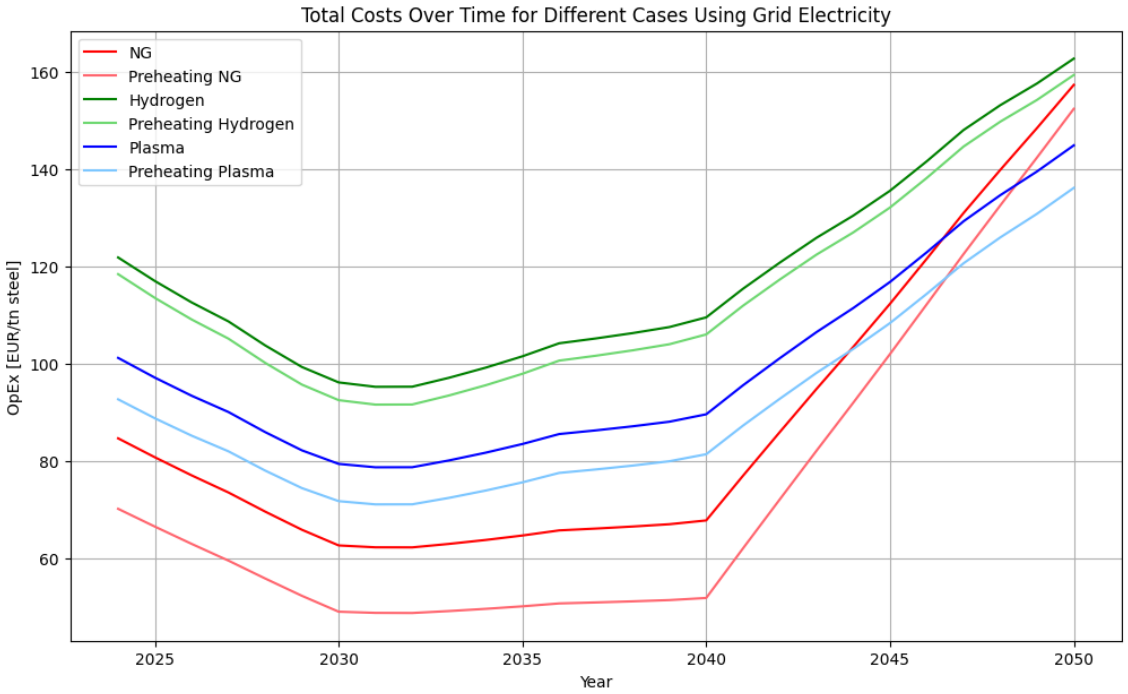

Figure 4.12: Operational Expenditure (OpEx) for Case GC

preheating a more cost-effective option than non-preheating. This is illustrated in Figure 4.13, which depicts the decomposed OpEx costs for all cases in the year 2024.

Figure 4.14 presents results analogous to those shown previously in Figure 4.12, with the focus now on the assessment of the RE scenario. The findings indicate that each electrification option demonstrates greater cost-effectiveness compared to the status quo technologies over time. This trend is attributed to the anticipated decline in the cost of renewable technologies in the coming years, particularly in the context of the Preheating Hydrogen Case.

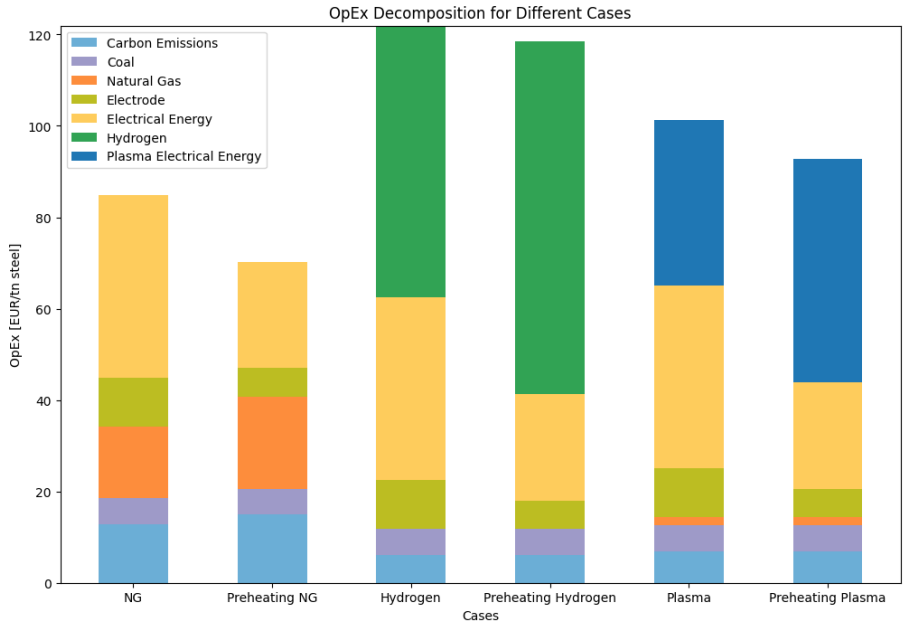

Figure 4.13: Decomposition of Operational Expenditure (OpEx) 2024

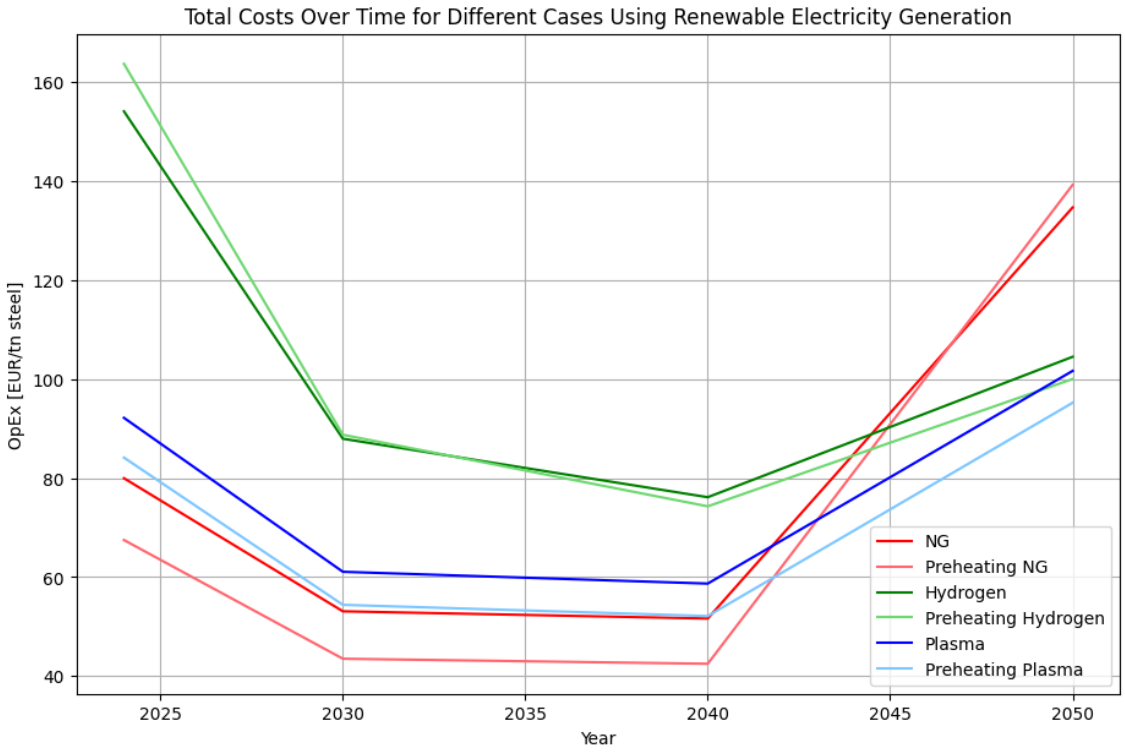

Figure 4.14: Operational Expenditure (OpEx) for Case RE

4.4.2 CapEx

As introduced in Section 4.4, CapEx refers to the investments a company makes to acquire, improve, or maintain physical and fixed assets. Effective CapEx management is critical to ensuring a company's long-term competitiveness and sustainability. This study evaluates the CapEx associated with a preheating furnace, plasma heating torch, Air Separation Unit (ASU), and electrolyzer.

The CapEx for a preheating furnace has been calculated for a capacity of 200,000 tons of steel per year. This cost was linearly extrapolated from the price of a preheating furnace with a capacity of 500,000 tons of steel per year, priced at 3,200,000 USD [65]

Similarly, the CapEx for the plasma torch system, including the air supply and cooling system, was extrapolated from a plasma torch capacity of 100 MW. This results in a specific price of 505 EUR per MW of installed capacity [66]. Additionally, the cost of installing a cryogenic air separation unit was considered, with the price calculated linearly using a rate of 187 EUR per ton of air processed annually [67].

For evaluating electrolyzer costs, Equation 58 was employed to determine the corresponding cost for the system. The price is dependent on the capacity of the electrolyzer required and the year of purchase.

$$C = (k_o + \frac{k}{Q}Q^{\alpha}) * (\frac{V}{V_o})^{\beta} \tag{58}$$

where:

- α = 0.622
- β = -158.9
- k_o = 585.85
- k = 9458.2
- V_o = 2020
- V = 2024

- Q = Electrolyzer Capacity [kW]

4.4.3 NPV

Since NPV evaluates the present value of expected cash flows by taking into account the time value of money, the results of NPV are determined not only by the cost of the project (OpEx & CapEx) but also by the inflation rate used to calculate NPV. For this study, an inflation rate of 3% was chosen.

The NPV has been calculated using equation 59.

$$NPV = \sum_{t=0}^{n} \frac{C_t}{(1+r)^t} \tag{59}$$

where:

- C_t = net cash inflow during the period t
- r = discount rate
- t = time period
- n = total number of periods

Since Case-1 (NG) represents the status quo technology, the NPV results are shown as a relative result from this case. Therefore, it is not the total NPV of the system that is discussed, but rather the difference in NPV from the status quo technology.

Figure 4.15 shows the results for the different scenarios in the GC configuration. The conclusion drawn from these results is that none of the electrification alternatives are cost-effective over the years if implemented from 2024. This is due to the fact that carbon prices are not yet significantly high, and grid electricity prices do not vary significantly over the years.

On the other hand, for the RE scenario, it can be seen from the results in Figure 4.16 that the electrification scheme with preheating plasma (Case-6) becomes increasingly cost-effective, along with the non-preheating plasma scheme (Case-5). By the year 2049, given the considered cost development and

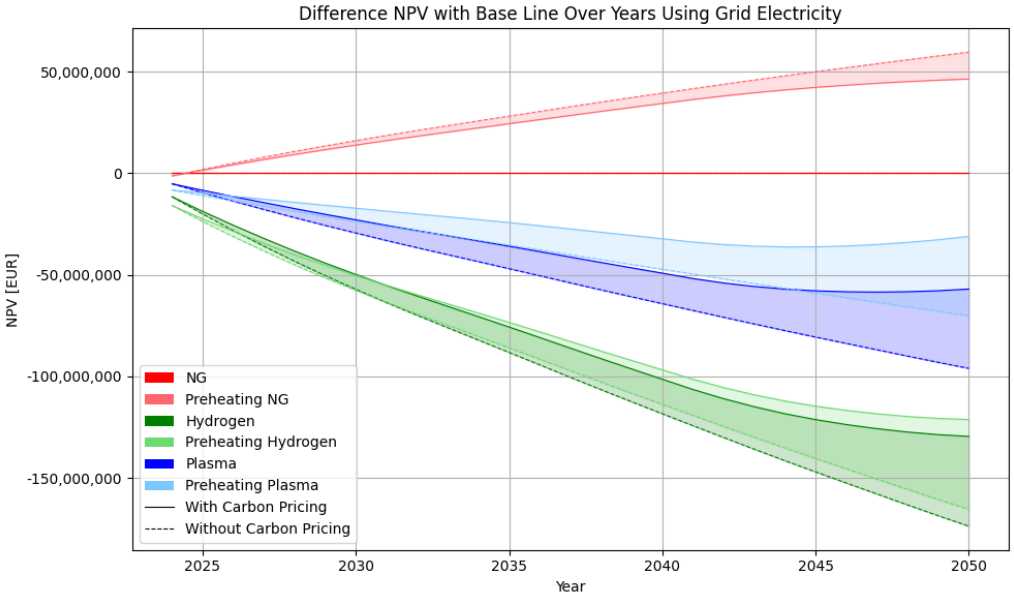

Figure 4.15: Net Present Value (NPV) results for Case GC

the implementation of carbon pricing, the Preheating Plasma scheme (Case-6) becomes cost-effective.

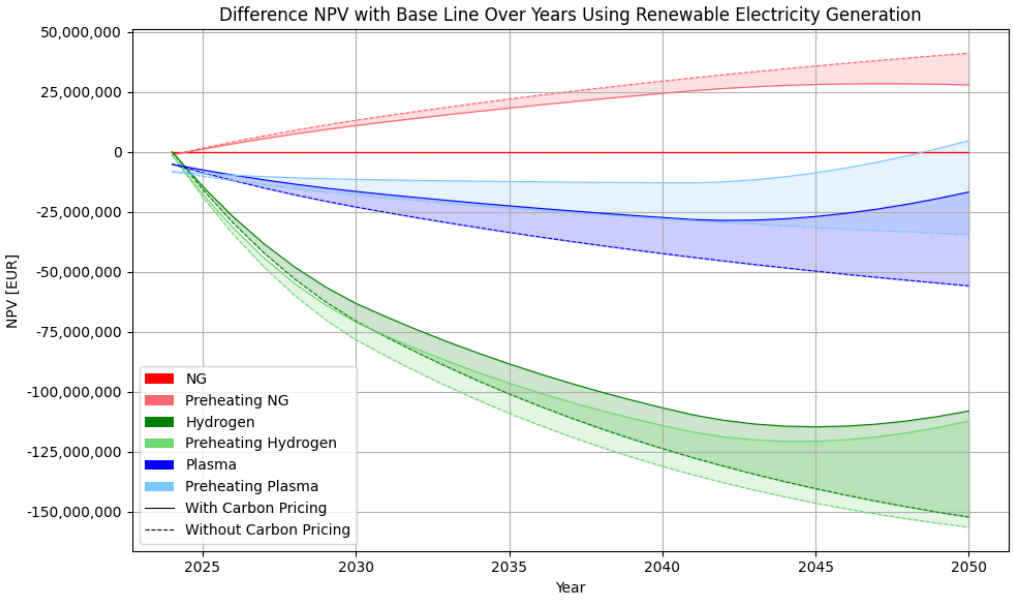

Figure 4.16: Net Present Value (NPV) results for Case RE

It can be concluded that for both cases, GC and RE, the electrification via hydrogen presents significant economic challenges, as the electrification option via plasma heating offers a more cost-effective solution. The results also demonstrate that without government intervention, green steel will not become cost-effective in

the future. This is primarily because the preheating schema using plasma heating technology only becomes cost-effective when economic analyses include carbon pricing.

5 Conclusions

This study has underscored the necessity to address the decarbonization of the steelmaking and post-processing phases, which have been largely overlooked in favor of the ironmaking phase. Through a comprehensive review and modeling of various decarbonization technologies, this research has demonstrated the potential for substantial emissions reductions and energy savings in these phases.

5.1 Answer to the research questions

In order to evaluate the study with the available data, the research questions identified in chapter 1 can be revised:

(1) *What technological advancements are necessary to decarbonize steel manufacturing, and how can they be implemented to reduce environmental impact?*

The steel industry can pursue decarbonization and electrification through several key approaches. Existing steel manufacturing plants, which have a significant remaining lifespan, can be retrofitted to reduce emissions without the need for complete reconstruction. Technologies such as Carbon Capture and Storage (CCS) and Carbon Capture and Utilization (CCU) are pivotal in this context. These technologies can significantly mitigate emissions by capturing and either storing or repurposing carbon dioxide produced during steel manufacturing.

For steel plants that are planned for construction in the near future, it is crucial to incorporate technologies with a high Technology Readiness Level (TRL) to ensure operational efficiency and sustainability. Implementing hydrogen combustion reheating furnaces or hydrogen-based shaft furnaces are viable options. These technologies leverage hydrogen as a cleaner fuel alternative, thereby reducing the carbon footprint of the steel production process.

The use of bioenergy occupies an intermediate position, as it can be utilized in existing steel plants. Although bioenergy has well-documented applications in other sectors, its impact on steel manufacturing is still under development and

requires further investigation.

For steel plants aiming to implement groundbreaking and disruptive technologies, options such as Hydrogen Plasma Smelting Reduction (HPSR), Molten Oxide Electrolysis (MOE), or Electrowinning present promising solutions. MOE, in particular, has the potential to drastically reduce emissions and transform the structural dynamics of steel plants by merging iron-making and steel-making process steps into one. These technologies represent significant advancements in the quest for sustainable steel production, offering substantial impacts on reducing the environmental footprint of the steel industry.

(2) *How does the electrification of steel manufacturing compare to traditional steel-making regarding energy consumption?*

A comparative analysis of the electrification options with the status quo technology revealed that all the electrification technologies under consideration are more energy-intensive than the status quo technologies. This is due to the fact that the electrification technologies studied require more process steps than the status quo technologies, resulting in a lower energy efficiency of the system. The generation of hydrogen and the need to achieve a plasma state are the primary factors contributing to the higher energy consumption associated with their processes. In the case of the EAF, the energy required to process H2-DRI in comparison to scrap-based EAF functionality is estimated to be 39% higher while, in comparison to DRI, the EAF consumes 4% more energy. It should be noted that the results from this particular study must be further complemented, and the energy required to process H2-DRI is expected to represent an even greater increase. On the other hand, the results of the electrification of the reheating furnace with hydrogen combustion indicate an expected increase of 71% in energy requirements while plasma heating represents an increase of 12%. This study is based on a pilot-scale study conducted by KTH, and further investigation into the implications of a large-scale plasma heating system would be necessary.

(3) *What are the economic implications of transitioning to electrified steel-making processes?*

The current cost-effectiveness of electrification technologies is hindered by the prevailing industry fuel costs and carbon pricing. The elevated operating expenses and considerable capital expenditures necessary to implement these technologies present significant obstacles to their widespread adoption. Furthermore, the current state of carbon pricing makes the integration of the green steel industry unfeasible in the near term. The principal factor driving the expansion of this industry is the demand for green steel. Nevertheless, this study posits that prospective implementation of carbon pricing may facilitate the cost-effectiveness of OpEx associated with electrification options, thereby potentially enhancing their adoption. It is important to note that this study exclusively considered costs, and thus did not consider scenarios in which revenues from increased steel prices would be higher. Moreover, the implementation of supportive policies and government financing could significantly facilitate the industry's transition, thereby aligning with the established EU decarbonization targets.

5.2 Future Work

This thesis has outlined several options for the decarbonization of mini-mills. However, further research is required to expand and refine these findings, addressing additional aspects that were beyond the scope of the present study.

As discussed in section 4.1, a major bottleneck of data regarding H2-DRI was found, which hinders the possibility to further analyze the impact of this metal on the energy consumption of the EAF. Furthermore, the EAF model could be complemented with further calculations in the energy transfer difference due to foamy slag and further decarbonization potential that has not been evaluated by replacing the injected coal in the EAF with biochar and evaluating the impact on the energy, decarbonization and economic analysis.

Regarding the following process steps in the mini-mill, the decarbonization technology of plasma heating has been developed from a pilot study developed at KTH and consideration of this on an industrial scale should be further investigated.

5.3 Summary

The study ultimately highlights the complexity of the steel industry and the multifaceted pathways that can be followed for its decarbonization. The comprehensive literature review encompassed the entirety of the steel industry, revealing significant momentum towards decarbonization through various approaches. In the modeling section of the thesis, the focus was placed on analyzing the mini-mill. Initially, the modeling of the EAF with different input metals demonstrated that future implementations of EAF's must carefully control energy inputs, as the introduction of new metal compositions significantly impacts the EAF's energy consumption. Subsequently, the mini-mill was analyzed as a whole, exploring its electrification using two distinct technologies: hydrogen combustion and plasma heating torches. The results indicated that utilizing clean electricity effectively mitigates emissions. However, the economic analysis revealed that, without policy intervention, the economic viability of sustainable steel production remains challenging.

References

[1] IEA. “Iron and Steel Technology Roadmap”. In: (2020). DOI: https://iea.blob.core.windows.net/assets/eb0c8ec1-3665-4959-97d0-187ceca189a8/Iron_and_Steel_Technology_Roadmap.pdf.

[2] Commission, European. “The European Green Deal Striving to be the first climate-neutral continent”. In: (2019). DOI: https://commission.europa.eu/strategy-and-policy/priorities-2019-2024/european-green-deal_en#:~:text=Learn%20how%20the%20EU%EE%80%80%20aims%20to%20become%20the%20first.

[3] Xin Wang Haitao Yang, Xiaohua Yu. “Research progress in the preparation of iron by electrochemical reduction route without CO2 emissions”. In: (2022). DOI: https://link.springer.com/content/pdf/10.1007/s10800-023-01870-7.pdf.

[4] Moya, Jose. “JRC Technical Report: Technologies to decarbonise the EU steel industry”. In: *European Commission* (2022). DOI: https://op.europa.eu/en/publication-detail/-/publication/fd3b326a-8aed-11ec-8c40-01aa75ed71a1/language-en.

[5] Kun Hea, Li Wang. “A review of energy use and energy-efficient technologies for the iron and steel industry”. In: *Renewable and Sustainable Energy Reviews* (2017). DOI: https://www.sciencedirect.com/science/article/pii/S1364032116310620?via%3Dihub.

[6] N. Schmitz, L. Sankowski. “Towards CO2-neutral process heat generation for continuous reheating furnaces in steel hot rolling mills – A case study”. In: *Energy* 224 (2021). DOI: https://www.sciencedirect.com/science/article/pii/S0360544221004047.

[7] Chakravarty, Koushik. “Increase in energy efficiency of a steel billet reheating furnace by heat balance study and process improvement”. In: (2020). DOI: https://www.sciencedirect.com/science/article/pii/S2352484719305815.

[8] Herbert Pfeifer, Marcus Kirschen. “Thermodynamic analysis of EAF electrical energy demand”. In: (2002). DOI: https://www.researchgate.net/publication/266466258_Thermodynamic_analysis_of_EAF_electrical_energy_demand.

[9] Wei, Guang-sheng. “Hybrid Modeling for Endpoint Carbon Content Prediction in EAF Steelmaking”. In: (2018). DOI: https://link.springer.com/chapter/10.1007/978-3-319-72131-6_19.

[10] Sanjal, Sujit. “The Value of DRI – Using the Product for Optimum Steelmaking”. In: (2015). DOI: https://www.midrex.com/tech-article/the-value-of-dri-using-the-product-for-optimum-steelmaking/.

[11] Memoli, Francesco. “Behavior and benefits of high-Fe3C DRI in the EAF”. In: (2015). DOI: https://www.researchgate.net/publication/282794593_Behavior_and_benefits_of_high-Fe3C_DRI_in_the_EAF.

[12] Hornby, Sara. “Hydrogen-Based DRI EAF Steelmaking — Fact or Fiction?” In: (2021). DOI: https://www.researchgate.net/publication/353328019_Hydrogen-Based_DRI_EAF_Steelmaking_-_Fact_or_Fiction.

[13] Nicolas Lalla, Luciana Pucchio. “INCREASING THE CARBON CONTENT IN DIRECT REDUCED IRON. CURRENT TRENDS, THERMODYNAMIC CALCULATIONS AND INDUSTRIAL RESULTS IN ARCELORMITTAL ACINDAR”. In: (2021). DOI: https://www.researchgate.net/publication/375126873_INCREASING_THE_CARBON_CONTENT_IN_DIRECT_REDUCED_IRON_CURRENT_TRENDS_THERMODYNAMIC_CALCULATIONS_AND_INDUSTRIAL_RESULTS_IN_ARCELORMITTAL_ACINDAR.

[14] Memoli, Francesco. “The use of DRI in a consteel® EAF process”. In: (2015). DOI: https://www.researchgate.net/publication/289506363_The_use_of_DRI_in_a_consteelR_EAF_process.

[15] Wang, R. R. “Hydrogen direct reduction (H-DR) in steel industry—An overview of challenges and opportunities”. In: (2021). DOI: https://www.sciencedirect.com/science/article/pii/S095965262103972X.

[16] Hornby, Sara. “Impact of Hydrogen DRI on EAF Steelmaking”. In: (2021). DOI: https://www.midrex.com/tech-article/impact-of-hydrogen-dri-on-eaf-steelmaking/.

[17] Ali Hasanbeigi Cecilia Springer, Hannah Irish. “Green H□-DRI Steelmaking: 15 Challenges and Solutions”. In: (2024). DOI: https://static1.squarespace.com/static/5877e86f9de4bb8bce72105c/t/663f2cc2c440a83768c59258/1715416296800/R6+Green+DRI+Steelmaking_.pdf.

[18] “Fact sheet: Scrap use in the steel industry”. In: *World Steel Association* (2021). DOI: https://worldsteel.org/wp-content/uploads/Fact-sheet-on-scrap_2021.pdf.

[19] Vogl, Valentin. “The making of green steel in the EU: a policy evaluation for the early commercialization phase”. In: (2020). DOI: https://www.tandfonline.com/doi/full/10.1080/14693062.2020.1803040.

[20] Muslemani, Hasan. “Opportunities and challenges for decarbonizing steel production by creating markets for ‘green steel’ products”. In: (2021). DOI: https://www.sciencedirect.com/science/article/pii/S0959652621023453.

[21] Ras, Kevin de. “Carbon capture and utilization in the steel industry: challenges and opportunities for chemical engineering”. In: *World Steel Association* (2019). DOI: https://www.sciencedirect.com/science/article/pii/S221133981930036X.

[22] Dora-Andreea Chisalita a, Letitia Petrescu a. “Assessing the environmental impact of an integrated steel mill with post-combustion CO2 capture and storage using the LCA methodology”. In: *Journal of Cleaner Production* 211 (2019). DOI: https://www.sciencedirect.com/science/article/pii/S095965261833659X.

[23] Simon Nicholas, Soroush Basirat. “Carbon capture for steel?” In: (2024). DOI: https://ieefa.org/resources/carbon-capture-steel.

[24] Voss, Andreas. “Injection of hydrogen into blast furnace: ThyssenKrupp Steel concludes first test phase successfully”. In: *thyssenkrupp Steel* (2021). DOI: https://www.thyssenkrupp-steel.com/en/newsroom/press-releases/thyssenkrupp-steel-concludes-first-test-phase-successfully.html.

[25] Pauna, Henri. “Hydrogen plasma smelting reduction process monitoring with optical emission spectroscopy – Establishing the basis for the method”. In: *Journal of Cleaner Production* (2022). DOI: https://www.sciencedirect.com/science/article/pii/S0959652622033327.

[26] Filho, Isnalsi R. Souza. “Green steel at its crossroads: Hybrid hydrogen-based reduction of iron ores”. In: *Journal of Cleaner Production* (2022). DOI: https://www.sciencedirect.com/science/article/pii/S0959652622004437.

[27] “voestalpine researching into hydrogen plasma for green steel production in an international showcase project”. In: *voestalpine* (2022). DOI: https://www.voestalpine.com/group/en/media/press-releases/2022-04-27-voestalpine-researching-into-hydrogen-plasma-for-green-steel-production-in-an-international-showcase-project/.

[28] “Our hydrogen plant”. In: *Ovako* (2023). DOI: https://www.ovako.com/en/about-ovako/our-hydrogen-plant/.

[29] Cavaliere, Pasquale. “Clean Ironmaking and Steelmaking Processes Efficient Technologies for Greenhouse Emissions Abatement”. In: (2019). DOI: https://link.springer.com/book/10.1007/978-3-030-21209-4.

[30] “Climate-neutral steelmaking in Europe”. In: *European Research Executive Agency* (2022). DOI: https://rea.ec.europa.eu/publications/climate-neutral-steelmaking-europe_en.

[31] Lupi, Sergio. “Fundamentals of electroheat: Electrical Technologies for Process Heating”. In: (2017). DOI: https://link.springer.com/book/10.1007/978-3-319-46015-4.

[32] Ilman Nuran Zaini a, Rikard Svanberg. “A pilot-scale test of plasma torch application for decarbonising the steel reheating furnaces”. In: *Thermal Science and Engineering Progress* 40 (2023). DOI: https://www.sciencedirect.com/science/article/pii/S2451904923001191#b0100.

[33] “Biomass applications in iron and steel industry: An overview of challenges and opportunities”. In: *Renewable and Sustainable Energy Reviews* (2016). DOI: https://www.sciencedirect.com/science/article/pii/S1364032116303896.

[34] “Torero: Replacing coal with sustainable, circular carbon in our steelmaking processes”. In: *ArcelorMittal* (). DOI: https://corporate.arcelormittal.com/climate-action/decarbonisation-technologies/torero-replacing-coal-with-sustainable-circular-carbon-in-our-steelmaking-processes.

[35] Bianco L.; Baracchini, G. “Sustainable Electric Arc Furnace Steel Production: GreenEAF”. In: (2013). DOI: https://www.iob.rwth-aachen.de/files/pub/Bianco_2013_postprint.pdf.

[36] Vito LOGAR, Dejan DOVŽAN. “Modeling and Validation of an Electric Arc Furnace: Part 1, Heat and Mass Transfer”. In: (2011). DOI: https://www.jstage.jst.go.jp/article/isijinternational/52/3/52_3_402/_pdf/-char/en.

[37] B. Wilthan, W. Schützenhöfer G. Pottlacher. “Thermal Diffusivity and Thermal Conductivity of Five Different Steel Alloys in the Solid and Liquid Phases”. In: (2015). DOI: https://link.springer.com/article/10.1007/s10765-015-1850-2.

[38] NIST. “NIST Chemistry WebBook, SRD 69, Nitrogen”. In: (2014). DOI: https://webbook.nist.gov/cgi/cbook.cgi?ID=C7727379&Type=JANAFG&Plot=on.

[39] NIST. “NIST Chemistry WebBook, SRD 69, Oxygen”. In: (2014). DOI: https://webbook.nist.gov/cgi/cbook.cgi?ID=C7782447&Mask=1.

[40] NIST. “NIST Chemistry WebBook, SRD 69, Carbon moxide”. In: (2014). DOI: https://webbook.nist.gov/cgi/cbook.cgi?ID=C630080&Mask=1F.

[41] NIST. “NIST Chemistry WebBook, SRD 69, Carbon dioxide”. In: (2014). DOI: https://webbook.nist.gov/cgi/cbook.cgi?ID=C124389&Mask=1#Thermo-Gas.

[42] NIST. “NIST Chemistry WebBook, SRD 69, Water”. In: (2014). DOI: https://webbook.nist.gov/cgi/cbook.cgi?ID=C7732185&Mask=1#Thermo-Gas.

[43] Marcus Kirschen a b Karim Badr b, Herbert Pfeifer a. “Influence of direct reduced iron on the energy balance of the electric arc furnace in steel industry”. In: *Energy* (2011). DOI: https://www.sciencedirect.com/science/article/pii/S036054421100524X.

[44] Vito LOGAR, Dejan DOVŽAN and ŠKRJANC, Igor. “Modeling and Energy Efficiency Analysis of the Steelmaking Process in an Electric Arc Furnace”. In: *ISIJ International* (2022). DOI: https://link.springer.com/article/10.1007/s11663-022-02576-5.

[45] K. C. Meher, N. Tiwari S. Ghorui. “Thermodynamic and Transport Properties of Nitrogen Plasma Under Thermal Equilibrium and Non-equilibrium Conditions”. In: (2015). DOI: https://link.springer.com/article/10.1007/s11090-015-9615-z.

[46] Statista. “Carbon intensity of the power sector in the European Union in 2023, by country”. In: (2023). DOI: https://www.statista.com/statistics/1291750/carbon-intensity-power-sector-eu-country/#:~:text=Poland%E2%80%99s%20power%20sector%20had%20the%20highest%20carbon%20intensity,carbon-intensive%20in%20the%20EU%2C%20producing%20just%2040.7%20gCO%E2%82%82%2FkWh..

[47] Sujay Kumar Dutta, Yakshil B. Chokshi. “Basic Concepts of Iron and Steel Making: Electric Furnace Processes”. In: (2020). DOI: https://link.springer.com/chapter/10.1007/978-981-15-2437-0_16.

[48] “The Influence of Electric-Arc-Furnace Input Feeds on its Electrical Energy Consumption”. In: (2021). DOI: https://link.springer.com/article/10.1007/s40831-021-00390-y.

[49] Vito Logar, Dejan Dovzan. “Modeling and Validation of an Electric Arc Furnace: Part 2, Thermo-chemistry”. In: (2012). DOI: https://www.researchgate.net/publication/233391600_Modeling_and_Validation_of_an_Electric_Arc_Furnace_Part_2_Thermo-chemistry.

[50] Eder Trejo, Fernando Martell. “MODELING OF POWER AND HEAT LOSSES OF ELECTRICAL ARC FURNACES”. In: (2010). DOI: https://www.eurosim.info/fileadmin/user_upload_eurosim/EUROSIM_OA/Congress/2010/data/papers/137.pdf.

[51] THOMAS MEIER, KARIMA GANDT. “Modeling and Simulation of the Off-gas in an Electric Arc Furnace”. In: (2017). DOI: https://www.jstage.jst.go.jp/article/isijinternational/52/3/52_3_402/_pdf/-char/en.

[52] National Academies of Sciences, Engineering and Medicine. “Health Risk Considerations for the Use of Unencapsulated Steel Slag”. In: (2023). DOI: https://www.ncbi.nlm.nih.gov/books/NBK599057/.

[53] Loredana Di Sante, F.Cirilli. “EAF slag: A product no longer a problem”. In: (2013). DOI: https://www.researchgate.net/publication/288731132_EAF_slag_A_product_no_longer_a_problem/figures?lo=1.

[54] Zinurov, Yuri N. Toulouevski Ilyaz Y. “Preheating of Scrap by Burners and Off-Gases”. In: (2009). DOI: https://link.springer.com/chapter/10.1007/978-3-642-03802-0_6.

[55] Agency, International Energy. “World Energy Outlook 2023”. In: (2023). DOI: https://iea.blob.core.windows.net/assets/86ede39e-4436-42d7-ba2a-edf61467e070/WorldEnergyOutlook2023.pdf.

[56] Economics, Trading. “EU Natural Gas TTF”. In: (2024). DOI: https://tradingeconomics.com/commodity/eu-natural-gas.

[57] statista. “Prices of electricity for non-household consumers with a consumption of 20,000 to 70,000 MWh in the European Union from 2008 to 2023”. In: (2024). DOI: https://www.statista.com/statistics/1046683/non-household-electricity-prices-european-union-eu/.

[58] Agency, International Energy. “Projected Costs of Generating Electricity”. In: (2020). DOI: https://iea.blob.core.windows.net/assets/ae17da3d-e8a5-4163-a3ec-2e6fb0b5677d/Projected-Costs-of-Generating-Electricity-2020.pdf.

[59] Observatory, European Hydrogen. “The European hydrogen market landscape”. In: (2023). DOI: https://observatory.clean-hydrogen.europa.eu/sites/default/files/2023-11/Report%2001%20-%20November%202023%20-%20The%20European%20hydrogen%20market%20landscape.pdf.

[60] Steelonthenet. “Steelmaking Electrode Prices”. In: (2024). DOI: https://www.steelonthenet.com/files/electrodes.html.

[61] Commission, European. “supplementing Directive 2003/87/EC of the European Parliament and of the Council concerning the determination of sectors and subsectors deemed at risk of carbon leakage for the period 2021 to 2030”. In: (2019). DOI: https://eur-lex.europa.eu/legal-content/EN/TXT/PDF/?uri=CELEX:32019D0708&from=EN.

[62] statista. “EU Carbon Permits”. In: (2024). DOI: https://tradingeconomics.com/commodity/carbon#:~:text=EU\%20carbon\%20permit\%20prices\%20fell\%20to\%20approximately\%20\%E2\%82\%AC67,thanks\%20to\%20ample\%20storage\%20and\%20decreased\%20regional\%20demand.

[63] Gabin MANTULET, Aurélien PEFFEN. “Carbon price forecast under the EU ETS”. In: (2023). DOI: https://www.enerdata.net/publications/executive-briefing/carbon-price-projections-eu-ets.html.

[64] Robert C. Pietzcker, Sebastian Osorio. “Tightening EU ETS targets in line with the European Green Deal: Impacts on the decarbonization of the EU power sector”. In: (2021). DOI: https://www.sciencedirect.com/science/article/pii/S0306261921003962.

[65] Agency, United States Environmental Protection. “AVAILABLE AND EMERGING TECHNOLOGIES FOR REDUCING GREENHOUSE GAS EMISSIONS FROM THE IRON AND STEEL INDUSTRY”. In: (2012). DOI: https://www.epa.gov/sites/default/files/2016-11/documents/iron-steel-ghg-bact-2012.pdf.

[66] Tadeusz M ˛aczka 1 Halina Pawlak-Kruczek 2, Lukasz Niedzwiecki 2. “Plasma Assisted Combustion as a Cost-Effective Way for Balancing of Intermittent Sources: Techno-Economic Assessment for 200 MWel Power

Unit". In: (2020). DOI: https://www.researchgate.net/publication/345465639_Plasma_Assisted_Combustion_as_a_Cost-Effective_Way_for_Balancing_of_Intermittent_Sources_Techno-Economic_Assessment_for_200_MWel_Power_UnitPlasma.

[67] technologies, Thunder Said Energy the research consultancy for energy. "Cryogenic air separation: costs and energy economics?" In: (). DOI: https://thundersaidenergy.com/downloads/cryogenic-air-separation-the-economics/.

[68] Matus Muron Grzegorz Pawelec, Daniel Fraile. "CLEAN HYDROGEN PRODUCTION PATHWAYS". In: (2024). DOI: https://hydrogeneurope.eu/wp-content/uploads/2024/06/2024_H2E_CleanH2ProductionPathwaysReport.pdf.

[69] Chiara Gulli Bernd Heid, Jesse Noffsinger. "Global Energy Perspective 2023: Hydrogen outlook". In: (2023). DOI: https://www.mckinsey.com/industries/oil-and-gas/our-insights/global-energy-perspective-2023-hydrogen-outlook.

[70] Peterseim, Jürgen. "Analysing the future cost of green hydrogen". In: (2022). DOI: https://www.pwc.com/gx/en/issues/esg/the-energy-transition/analysing-future-cost-of-green-hydrogen.html#:~:text=Hydrogen%20production%20costs%20will%20decrease%20by%20around%2050%25,Australia%20will%20be%20in%20the%20range%20of%20%E2%82%AC1%2Fkilogram..

[71] Zhou, Huangluolun. "Update: EU Energy Outlook 2050 – How will Europe evolve over the next 30 years?" In: (2021). DOI: https://blog.energybrainpool.com/en/update-eu-energy-outlook-2050-how-will-europe-evolve-over-the-next-30-years/.

Appendices

Appendix - Contents

A LCOH in Europe for GC and RE scenarios **79**

B Forecasted OpEX costs **80**

A LCOH in Europe for GC and RE scenarios

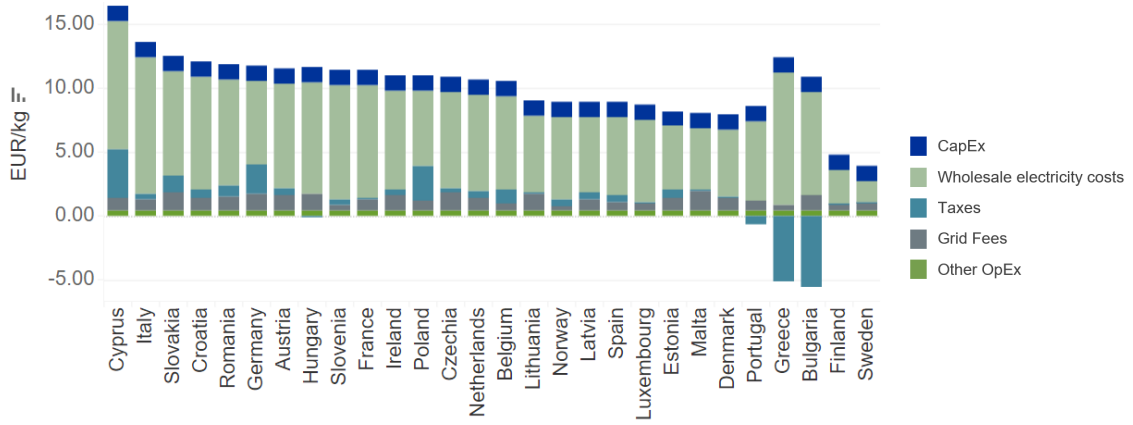

Figure A.1: Levelized Cost of Hydrogen in Europe for Grid-connected electrolysis

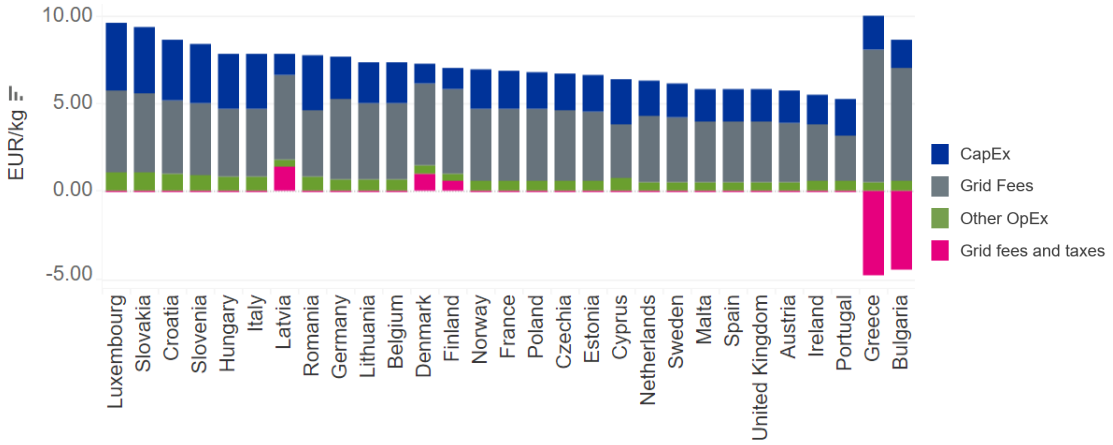

Figure A.2: Levelized Cost of Hydrogen in Europe for renewable hydrogen

As discussed in Section 4.4, the profitability of both the GC and RE hydrogen production scenarios largely depends on the region in which the steel plant is located. For instance, in Sweden and Finland, hydrogen production through the GC scenario proves more cost-effective. However, in the majority of EU countries, the RE scenario offers a more economical solution for hydrogen generation.

This also demonstrates that the implementation of policies to make the green steel industry economically viable can come from various approaches. For instance, subsidies for the use of hydrogen, as seen in Greece and Bulgaria, significantly impact the final price of hydrogen. These policies complement the strategy of increasing carbon pricing, providing a multifaceted approach to support the transition to sustainable steel production.

B Forecasted OpEX costs

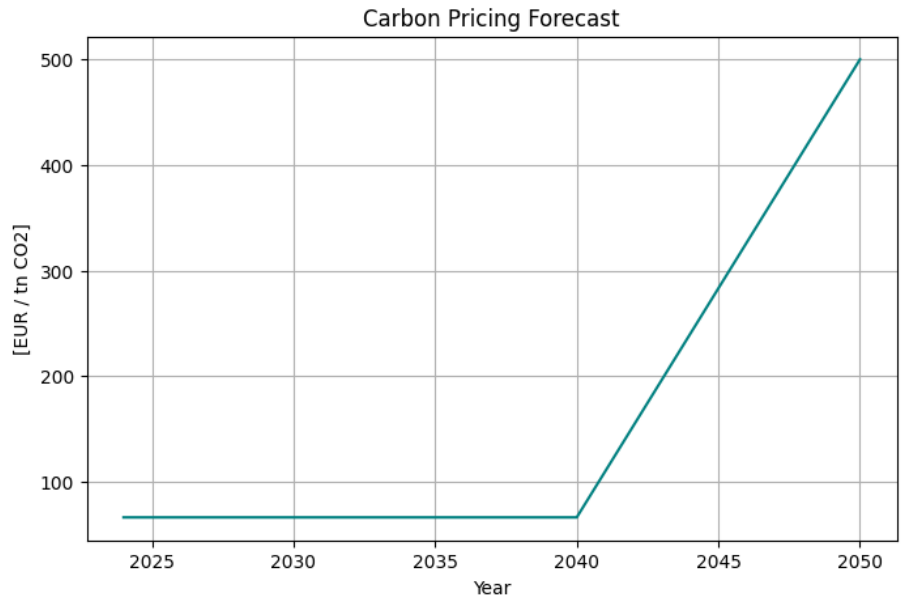

Figure B.1: Projected EU ETS Trend [64]

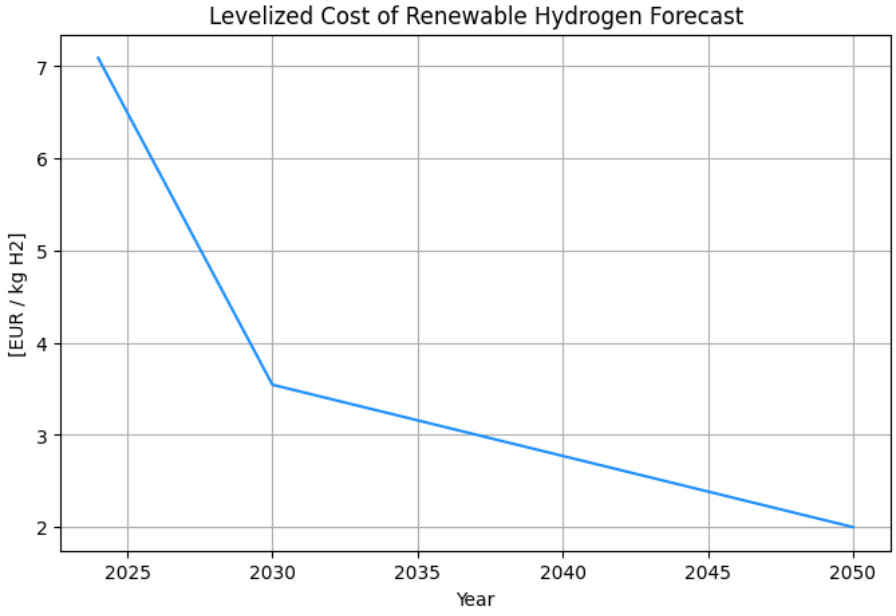

Figure B.2: Projected LCOH in Europe [68], [69], [70]

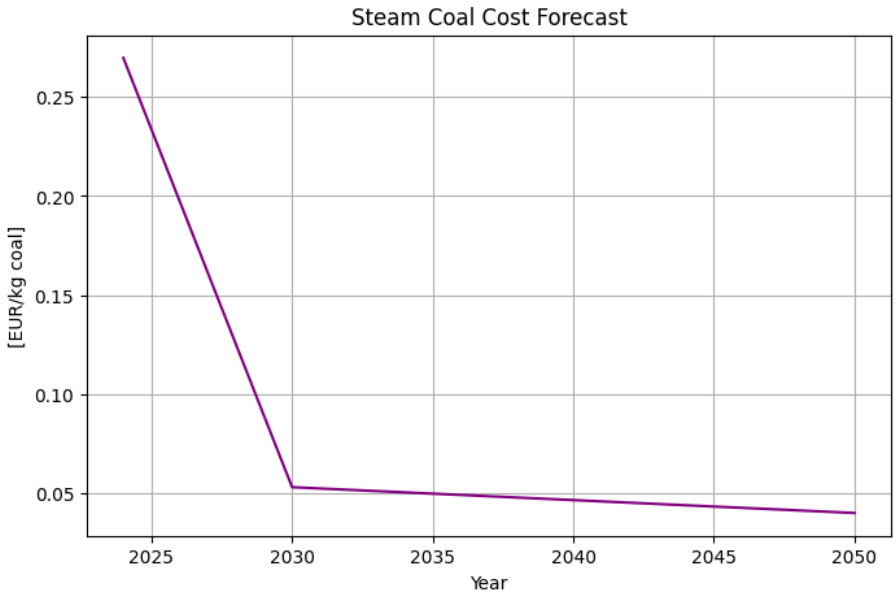

Figure B.3: Projected Cost of Steam Coal in Europe [55]

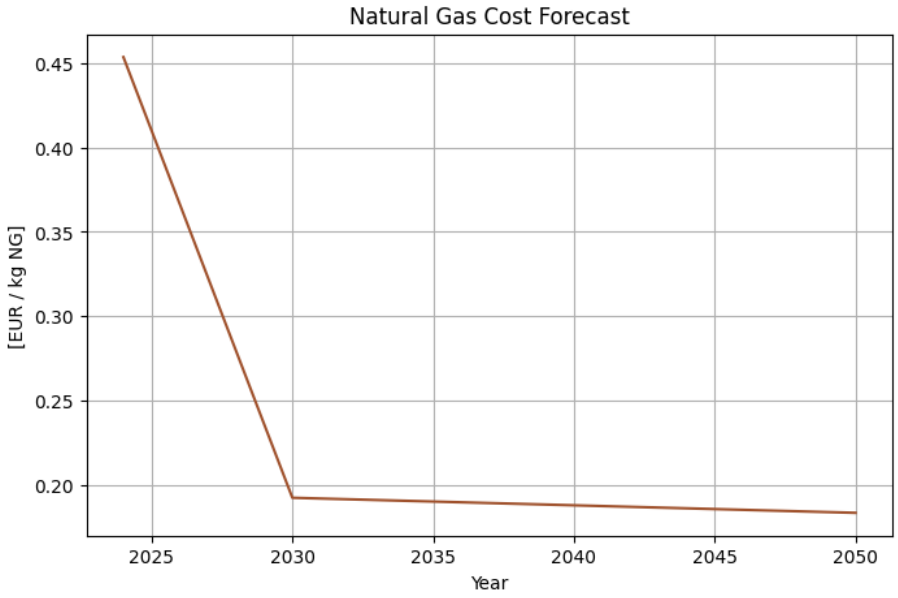

Figure B.4: Projected Cost of Natural Gas in Europe [55]

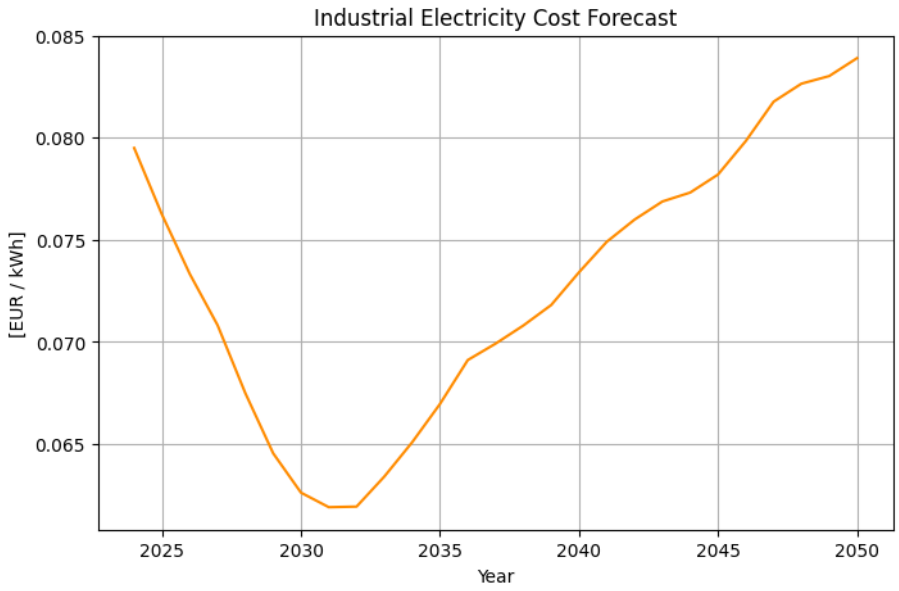

Figure B.5: Projected Industrial Electricity Prices in Europe [71]

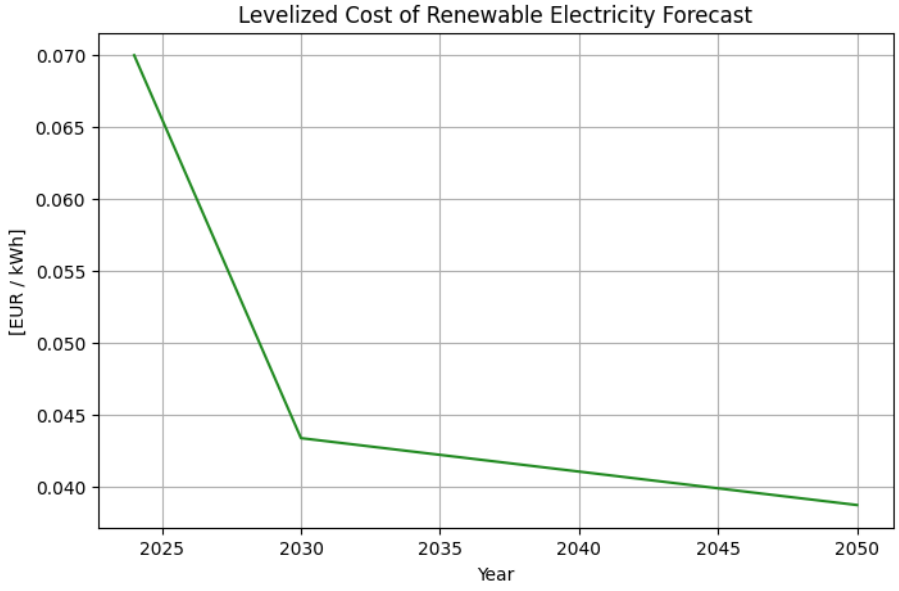

Figure B.6: Projected LCOE in Europe [55]